AD 296 436

NAVWEPS REPORT 7889
NOTS TP 2882
COPY 91

A STUDY OF UNDERWATER ACOUSTICAL IMAGING

by

E. E. Curry
Test Department

ABSTRACT. TV-like pictures, showing position and shape of underwater missile test items are obtained by using a directional-scanning sonar method. This report is a systems study made to investigate the problems of acoustical imaging within the broad concept of such an instrumentation device. It covers the interrelationship of absorption, bandwidth, information-theory limits, and beam theory for transducers and acoustical lenses.

U.S. NAVAL ORDNANCE TEST STATION

China Lake, California

November 1962

U. S. NAVAL ORDNANCE TEST STATION

AN ACTIVITY OF THE BUREAU OF NAVAL WEAPONS

C. BLENMAN, JR., CAPT., USN
Commander

WM. B. MCLEAN, PH.D.
Technical Director

FOREWORD

This study is part of the U. S. Naval Ordnance Test Station's underwater instrumentation-development program at San Clemente Island to obtain position/shape information on underwater missile test items. The report is intended for technical personnel involved in underwater instrumentation work at NOTS and at other underwater test range centers.

The work was performed during calendar year 1961, and was supported by Task Assignment R36R-IN 307/216-1/F099-03-003 and SP 24401.

This report has been reviewed for technical accuracy by Loran McCormick and H. L. Bagge.

F. M. ASHBROOK, Head
Instrument Development Division

Released under
the authroity of
IVAR E. HIGHBERG, Head
Test Department

ACKNOWLEDGMENT

The author wishes to thank Loran McCormick for his assistance in the experimental work covered by this report. In addition, Appendices B and C were written by Mr. McCormick.

NOTS Technical Publication 2882
NAVWEPS Report 7889

Published by . . . . . Test Department
Manuscript 30/MS-499
Collation . . . . . Cover, 22 leaves, abstract cards
First Printing . . . . . 225 numbered copies

CONTENTS

Figures:

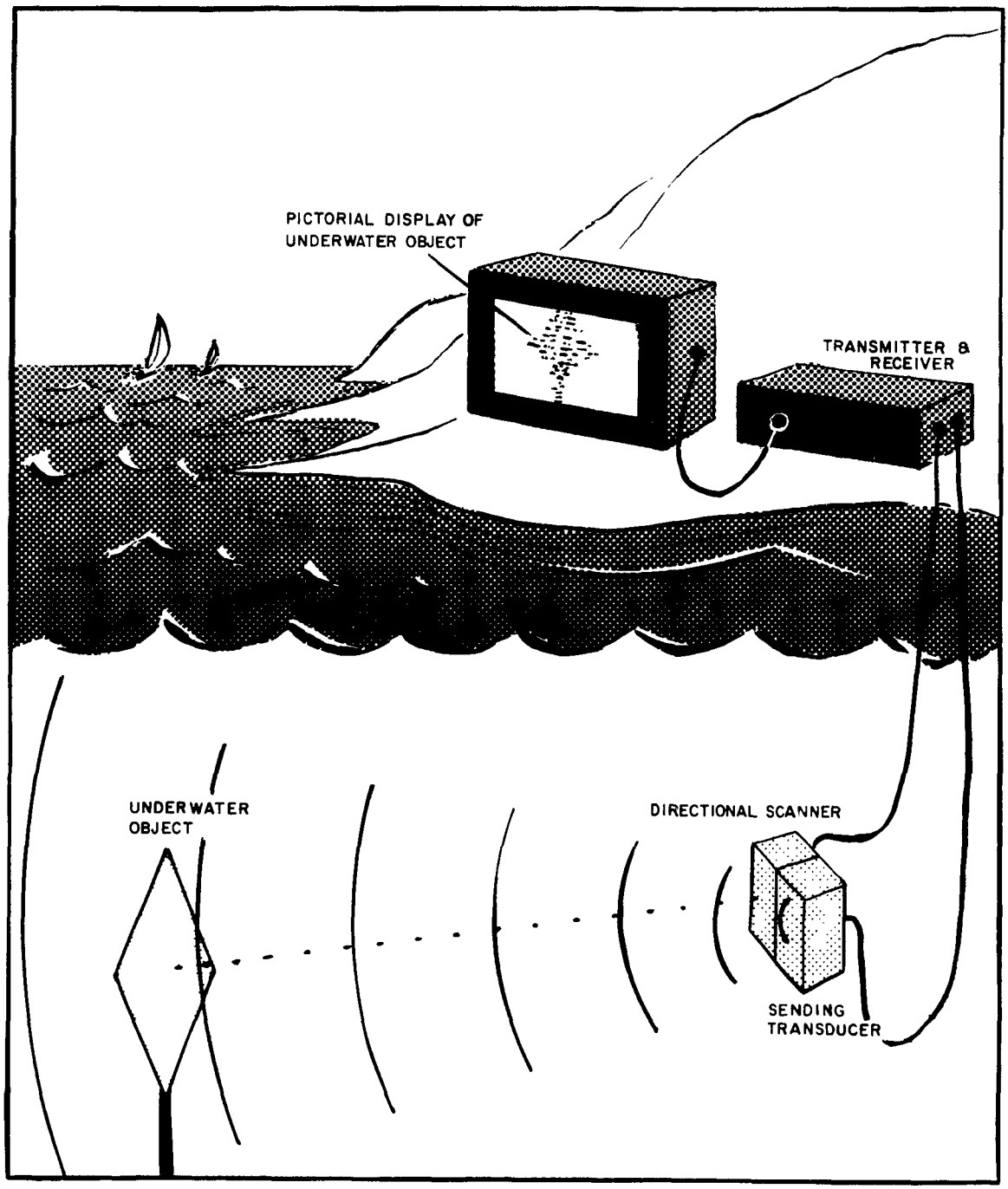

Schematic of Acoustical Imaging Concept.

INTRODUCTION

This study was made to determine the extent to which acoustical techniques can be used to obtain underwater information (such as position, size, and shape of test items) at distances greater than those currently obtainable by optical methods. The approach pursued was to try to present acoustical images as two-tone pictures on an oscilloscope, thus combining some of the features of both directional-scanning sonar and television. It was proposed to achieve this by transmitting a wide-angle, high-energy, long-duration pulse, and scanning the area with a narrow-beam receiving-transducer system. Then (depending on the system) the signal would be switched if necessary, and amplified to present the picture for viewing.

The sequence of pulse duration and scan time was investigated to determine bandwidth requirements as a function of resolution.

The study of the Mills cross approach was undertaken because it was believed the beam pattern of the Mills cross was the product of the patterns of the two line arrays. It was further believed that this concept could be expanded into a beam-switching Mills cross. When tests with the Mills cross indicated low contrast, a study of beam patterns was made starting with simple line transducers, then continuing to the Mills cross, and, finally, to the switching Mills cross.

A lens system study was then made to determine if such a system would produce better contrast; lens tests were conducted to verify the results.

Appendix A includes calculations on transmission losses, Appendix B is a report on studies of circuit noise, and Appendix C describes high-frequency commutating (switching) techniques.

Each phase of this study is more fully described under appropriate headings throughout the text of the report.

TIME FUNCTION AND BANDWIDTH

Transmission time considerations include scan time, bandwidth, zone of coverage, and pulse duration. The scan time is a function of area, resolution, and bandwidth. The depth of field (or zone of coverage) is a function of pulse duration and scan time. Note that in the examination of these time functions and their corresponding distances there is a two-way time factor involved, i.e., the time it takes the pulse to travel to the point of interest and return to the receiving transducer.

The signal must be transmitted for some time, t_t, which is a function of the scan time, t_s, and the depth of field, D_F. The speed of sound in water is c. Therefore,

$$t_t = t_s + \frac{2\ D_F}{c}\ , \text{ and}$$

$$t_s = \frac{2\ D_s}{c}$$

There is a minimum distance, D_d, which must be compatible with the system; thus,

$$D_d = \frac{t_d\ c}{2}$$

where t_d is the time of delay after transmitting until start of scan. Sketch 1 shows the zone of coverage:

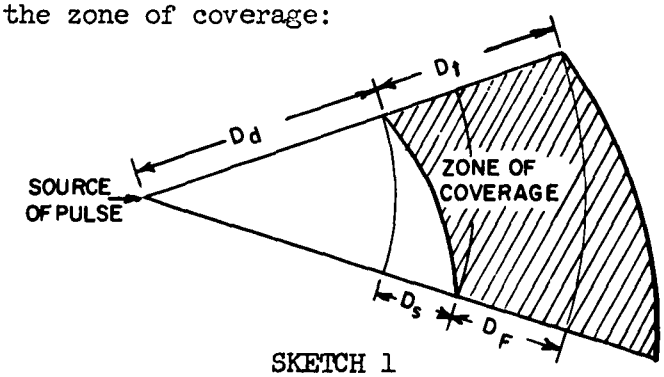

SKETCH 1

Since acoustical transmission and low-level reception are probably not possible at the same time, the transmit time may not be greater than the receive time, and reception must be done during the delay time between transmit pulses.

Multiple scan, interlacing of the scan, and multiple pulse alter the zone of coverage. All of these techniques are available for use in acoustical imaging systems.

The resolution and area coverage determine the number of bits of information per frame. The time of scan is determined by this and the maximum rate of information flow.

Sampling and switching functions require some bandwidth, W. Then the binary-channel capacity, C, is derived by, (Ref. 1):

$$C = W\ \text{Log}_2\ (1 + \frac{S}{N}), \qquad \text{where} \qquad \frac{S}{N} = \text{signal to noise ratio}$$

$$\text{when } \frac{S}{N} = 1, \quad \text{then}$$

$$C = W$$

This equation represents the upper limit of information theory, so compromises must be considered as functions of this maximum rate of information flow.

There is a Doppler shift of the received signal related to the velocity of the target and to the signal source, which increases the bandwidth requirements. The following calculations (together with calculations to combine constants) are necessary to arrive at a constant--referred to here as the Doppler-shift constant.

$$\text{Doppler shift} = \frac{2v}{\lambda}$$

$$= \frac{2v}{\frac{c}{f}} = \frac{2vf}{c}$$

$$= KVF$$

Doppler shift, given in cps
v = relative velocity, fps
λ = wavelength, ft
c = speed of sound, fps
f = frequency of signal, cps
K = conversion constant
V = relative velocity, nautical mph
F = frequency of signal, kc

Therefore, Doppler shift equals

$$K = \frac{2V\ (6080)\ F\ (1000)}{(5000)\ (3600)}$$

$$K = .675\ \frac{\text{cps/knot}}{\text{kc}}$$

TRANSMISSION AND ABSORPTION

In this section, it is intended to treat acoustical transmission and absorption of acoustical energy in a water medium. In the calculations presented some assumptions are made that will imply specific imaging devices. The purpose of this study is to investigate the problems involved.

For range calculations the log system of decibels is used with a reference pressure of 1 μb = $\frac{1\ \text{dyne}}{\text{cm}^2}$ (1,013.3 mb are equal to one standard atmosphere of pressure), Ref. 2.

The onset of cavitation, which occurs in water when certain intensities are exceeded, limits the maximum power per unit area transmitted through the water. Existing literature does not reveal a sharply-defined upper limit for these intensities since other factors (i.e., length of pulse, depth of water, and amount of air in solution), affect the maximum intensity. For example, with air-saturated water the intensity limit is less than 2 watts/sq cm. For sea water, the intensity limit covers a range from 0.2 to 2.0 watts/sq cm, Ref. 3. The estimated limit for a long-pulse source at a depth of 6 feet or more is 0.5 to 1.0 watt/sq cm.

A sending transducer probably should be a large segment of a sphere, perhaps 20° x 20°, capable of transmitting 1,000 watts of acoustical power since the power requirements call for a large surface area. A flat transducer is not satisfactory since it would have a narrow beam, which would make some method of focusing the energy to a diverging beam necessary.

Based on a conservative estimate of intensity limit, the surface area of the transducer should be 2,000 sq cm, or about 18 inches on each side.

$$r = \frac{18 \text{ in.}}{\theta} = \frac{18 \text{ in.}}{\frac{20^\circ}{57.4^\circ/\text{rad}}}$$

θ = central angle of transducer in radians
r = radius of transducer

$$= 51.6 \text{ inches} = 4.3 \text{ feet}$$

and

$$P = \sqrt{\rho c \, I \, 10^7}$$

$$= 8.8 \times 10^5 \mu b$$

or +119 db

I = intensity (average), watts/cm^2 = 0.5 watts/cm^2
P = pressure
ρ = density, grams/cm^3
c = speed of sound, cm/sec
ρc of water = 154,000 dynes/cm^2

Since the reference is in decibels, a shift from 1,000 watts to 100 watts would be only -10 db, or a shift from 119 to 109 db.

Radiated power varies inversely to the square of the distance, because of spreading. For simple calculations the center of the sphere becomes the imaginary source of the 20 x 20° beam. In addition, a flat object, with good reflection characteristics, is used to reflect the beam; thus the spreading of the energy returning along the two-way distance is equal to twice the one-way traveling distance. This becomes a power factor of 1/4, or -6 db. Spreading and absorption at several frequencies along the two-way distance are presented in Fig. 1. Absorption constants for absorption in water are shown in Fig. 2. The data for Fig. 2 was computed from information appearing on p. 3-71, Ref. 4.

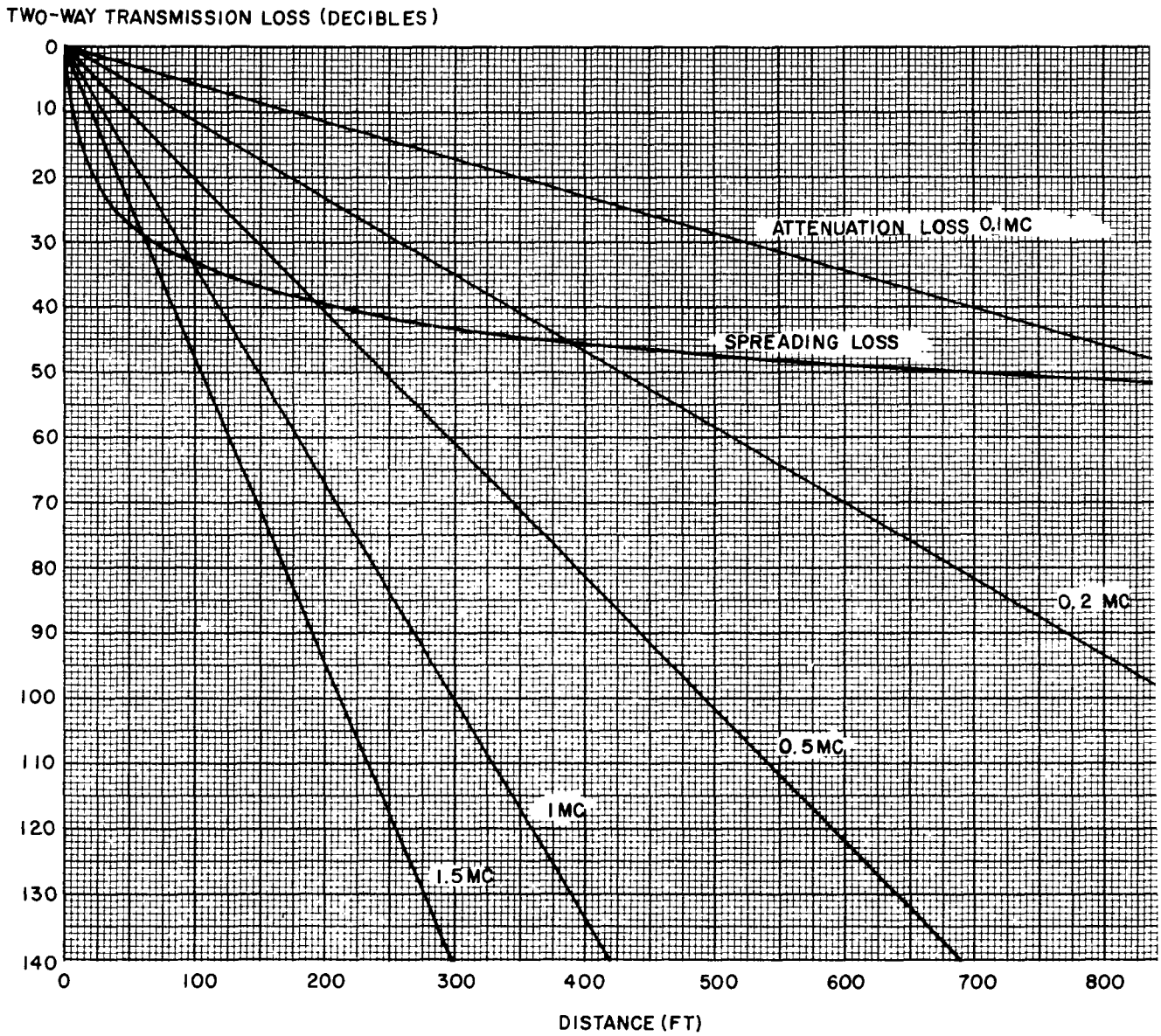

FIG. 1. Transmission Losses.

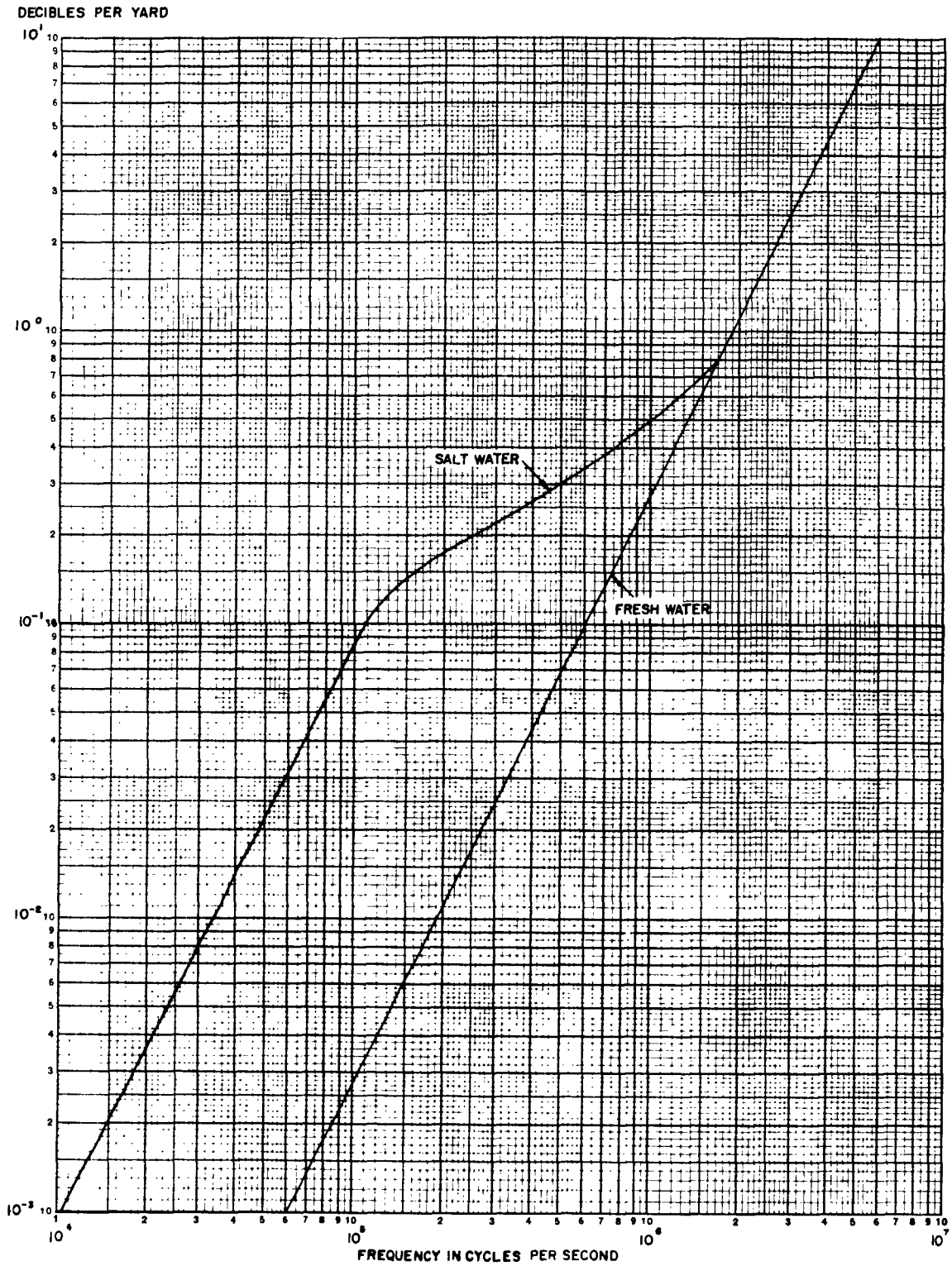

FIG. 2. Sound Absorption Functions for Water and Seawater.

To calculate the spreading loss for the transducer with a radius of curvature of 4.3 feet for one point 50 feet away (or a two-way distance of 100 feet:

$I_1 A_1 = I_2 A_2$

$A \propto r^2$

$$\frac{I_1}{I_2} = \left(\frac{d_2}{d_1}\right)^2$$

$$= \left(\frac{4.3}{100}\right)^2$$

$= -27$ decibels.

I_1 = intensity at transducer

I_2 = intensity at twice distance of interest

A_1 = area of transducer

A_2 = area of beam at distance of interest

d_2 = twice distance of interest

d_1 = radius of curvature of transducer

The spreading loss may be calculated by this method for any angle of coverage. (Note that this method of calculation keeps the reference point behind the transducer at its spherical center and that the intensity has been calculated on the front surface of the transducer instead of one yard in front of the transducer, as is the standard practice.) The returning signal intensity will be of a very low amplitude, i.e., the pressure-wave amplitude might be as low as 0 to -40 decibels. Thus,

$$P = \sqrt{\rho c\ I \times 10^7}$$

$$I = \frac{P^2\ 10^{-7}}{\rho c}$$

at P = 0 db, or 1 μb

$$I = \frac{10^{-7}}{1.54 \times 10^5}$$

$$= 6.5 \times 10^{-13} \text{ watts/cm}^2$$

P = pressure, dynes/cm^2

ρ = density, grams/cm^2

c = speed of sound, cm/sec

I = intensity, watts/cm^2

Therefore,

at 0 db	I is	6.5	10^{-13}	watts/cm^2
-10		6.5	10^{-14}	watts/cm^2
-20		6.5	10^{-15}	watts/cm^2
-30		6.5	10^{-16}	watts/cm^2
-40		6.5	10^{-17}	watts/cm^2

MILLS CROSS TRANSDUCER

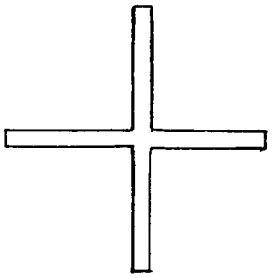

SKETCH 2

The Mills cross transducer is a cross of two line arrays of antennas used to achieve a directional antenna system. In this report a Mills cross refers to crossed line acoustical transducers in directional acoustical transducer arrays. See Sketch 2.

If eight barium titanate transducers, each 0.150 inches by 3.0 inches at 1.5 Mc, with the outside four being shaded to about one half their driving current, are used, the effective area will be about 2.7 sq in. = 17.4 cm^2 with an input impedance of about 5 ohms. The electrical power available, if properly coupled (impedance matched), is one-half the power in the receiving transducer times some efficiency factor, K. A value of K, 0.1, has been established for calculating the available power, W. Thus, for a pressure reference level of 0 db:

$$W = 1/2\ K\ I\ A$$

$$W = 0.5\ (0.1)\ 6.5 \times 10^{-13}\ (17.4)$$

and $W = 5.65 \times 10^{-13}$ watts

W = available power, watts
K = efficiency factor
I = intensity, watts/cm^2
A = area, cm^2

For a pressure reference level of -20 db:

$W = 5.65 \times 10^{-15}$ watts, and

for a pressure reference level of -40 db:

$W = 5.65 \times 10^{-17}$ watts.

If an impedance-matching device has no loss, then the voltage for a 1,000-ohm load is:

$$E = \sqrt{WR}$$

E = voltage, volts
W = power, watts
R = resistance, ohms

For a 0-db pressure reference level:

$E = 2.38\ 10^{-5}$ volts,

for a pressure reference level of -20 db:

$E = 2.38\ 10^{-6}$ volts, and

for a pressure reference level of -40 db:

$E = 2.38\ 10^{-7}$ volts.

If no matching device is used and the load is large, the one-half-power transfer factor is dropped. Now the 0-db pressure-reference level voltage across the 5-ohm transducer is:

$$E = \sqrt{11.3 \times 10^{-13} \times 5} = 2.38\ 10^{-6} \text{ volts}$$

From this voltage the lower limit of reception can be estimated in the range of 0 to -20 db if 1 μvolt is the minimum signal that can be detected.

BEAM CALCULATIONS FOR LINE TRANSDUCER

Small increments of the incoming signal are added vectorially when a line transducer, such as one line of a Mills cross, is used. Thus a long-line transducer, receiving a pressure wave in phase at all points, will produce a maximum signal output.

A source at such a distance that it would produce a curved wave front can be considered to be in the near field of the transducer (see Sketch 3). A curved transducer then could be used to increase the signal, and can be considered to have a focussed effect for a distance equal to the radius.

The nulls for a line transducer would be formed at an angle where the received signals would be completely canceled, and the side lobes would be formed at an angle of maximum signal. The first side lobe, then, could be represented as shown in Sketch 4.

The strength of the signal arriving at the transducer at angle θ (the first side lobe as shown in Sketch 4) may be calculated by summing the pressure, P, over the area of the transducer. Therefore, using x to denote distance along the transducer of length, ℓ, and assuming unity width, w, the average amplitude of pressure relative to the peak is:

$$\frac{P\ av}{P\ max} = \left[\int_0^{3\pi} \frac{w \sin x\ dx}{w\ 3\pi} \right] \cos \theta$$

The cos θ term is needed to give the effective vertical pressure on the transducer. For example, using a long-line transducer, 200 wavelengths long:

$$\theta = \sin^{-1} \frac{\lambda}{(2/3)\ 200\lambda} = 0.430, \quad \text{therefore } \cos \theta \cong 1.$$

Thus, let cos θ = 1,

$$\frac{P\ av}{P\ max} = \int_0^{3\pi} \frac{\sin x\ dx}{3\pi} = 0.212$$

$$= -13.5 \text{ db}$$

A quick and simple way to find the pressure on the above transducer is to add the increments of pressure over the surface of the transducer. One sine wave adds to zero. The average value of one-half sine wave is 0.636 of the peak value; this is over one-third of the area of the transducer.

$$P\ av = \frac{(\text{pressure})\ (\text{length})\ (\text{width})}{(\text{length})\ (\text{width})} = \frac{P\ max\ (0.636)}{3}\ 1$$

$$\frac{P\ av}{P\ max} = -13.5 \text{ db}$$

The first null could be represented by the pressure wave hitting the transducer so that the signal sums to zero, as shown in Sketch 5.

These values of θ could be calculated for a shaded transducer; however, the Tables in Ref. 5 are used since these values have already been calculated.

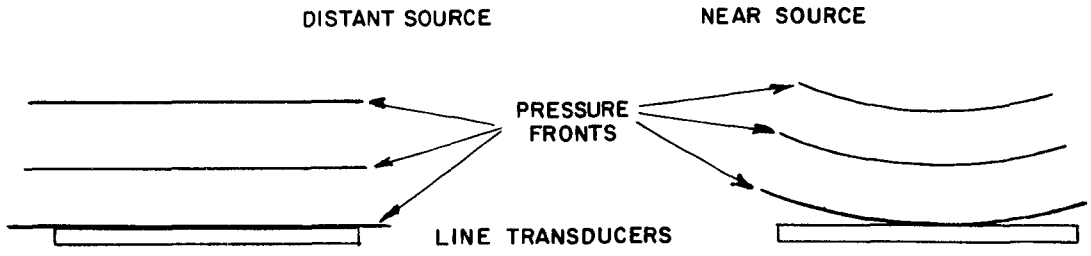

SKETCH 3

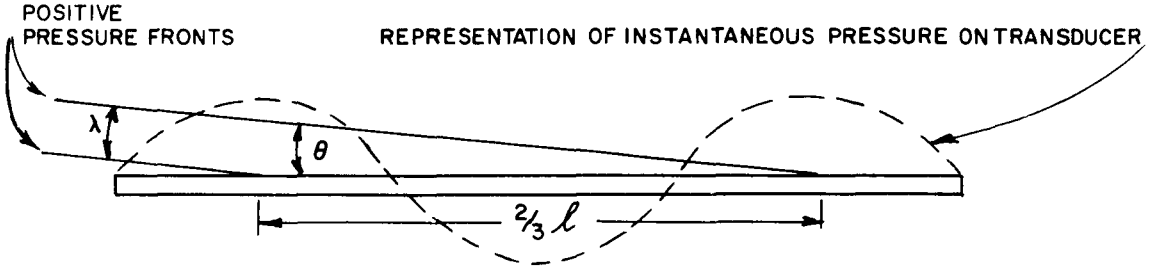

SKETCH 4

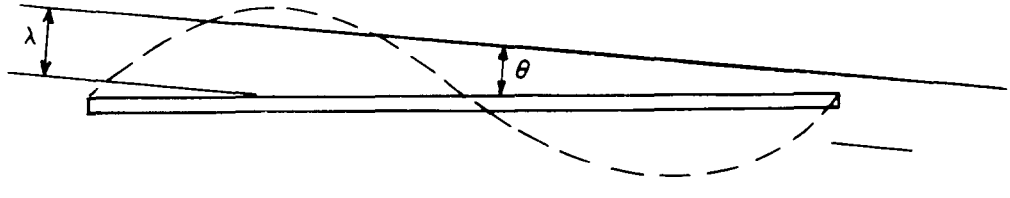

SKETCH 5

BEAM CALCULATIONS FOR MILLS CROSS TRANSDUCER

Now we can examine the Mills cross transducer in terms of this method. First we examine the angle that represents a null on one transducer and full signal on the other, as shown in Sketch 6.

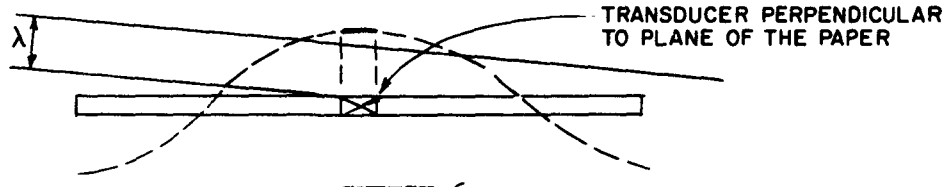

SKETCH 6

The average pressure of the Mills cross transducer equals the mean of the average value on each of the two line arrays.

$$P_{av} = \Sigma P_{max}\ 1/2\ (1 + 0)$$

$$\frac{P_{av}}{P_{max}} = -6 \text{ db}$$

Thus a null on one transducer will constitute a 6 db loss for the complete cross.

The first side lobe on one transducer can now be calculated, see Sketch 7.

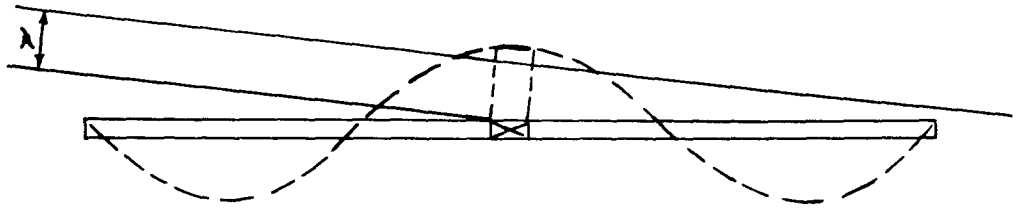

SKETCH 7

$$P_{av} = \Sigma P_{max}\ 1/2\ (1 - 0.212)$$

$$\frac{P_{av}}{P_{max}} = 0.394 = -8 \text{ db}$$

For the second side lobe:

$$P_{av} = \Sigma P_{max}\ 1/2\ \left(1 + \frac{0.636}{5}\right)$$

$$\frac{P_{av}}{P_{max}} = 0.56 \quad = \quad -5 \text{ db}$$

The fields of the line arrays of a Mills cross transducer with some values for combined signals are shown in Sketch 8:

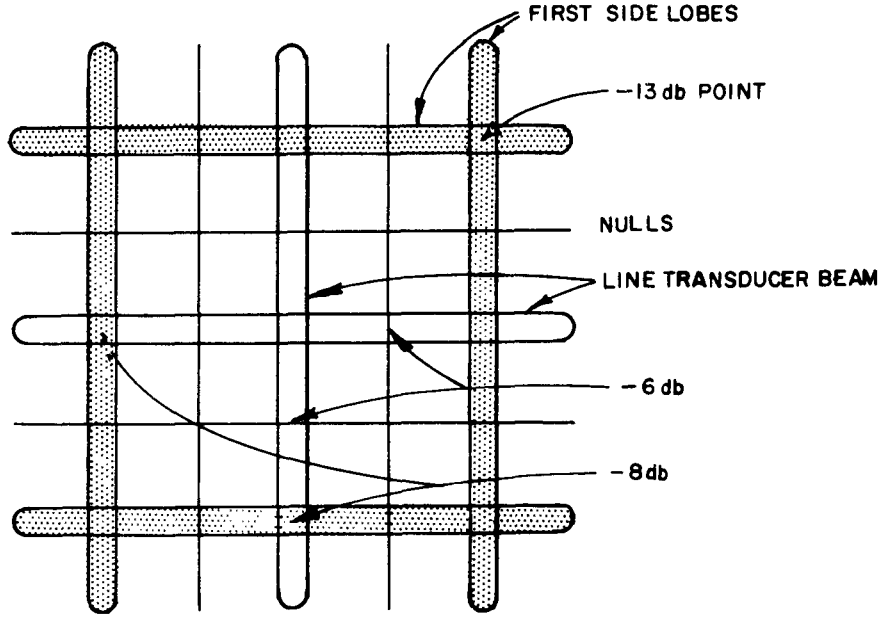

SKETCH 8

Sketch 9 shows amplitude sketched against angular displacement. Each fan of the X-shaped sensitivity pattern is the fan of one line of a Mills cross transducer, and is about 20° wide.

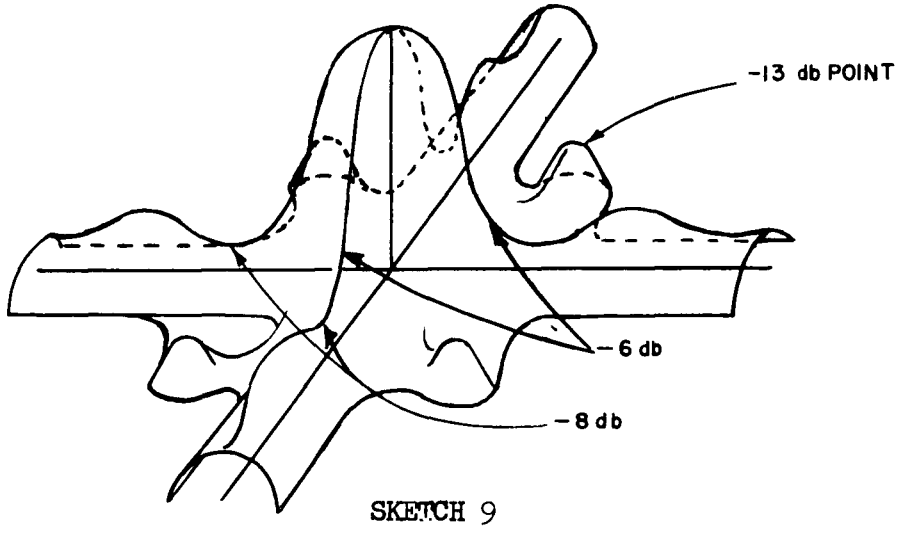

SKETCH 9

BEAM CALCULATIONS FOR MILLS CROSS SWITCHING TRANSDUCER

The expanded concept of switching in different directions by monitoring different elements will be referred to as a Mills cross switching transducer. If such a switching transducer is constructed to switch through 20°, each element must be long and narrow--200 to 300 wavelengths long* (depending on the shading), Ref. 5, and not more than $2\frac{1}{2}$ wavelengths wide.

A Mills cross switching transducer might be any of several configurations (see Figs. 3 and 4). Problems which might be anticipated will vary with the physical configuration of each transducer.

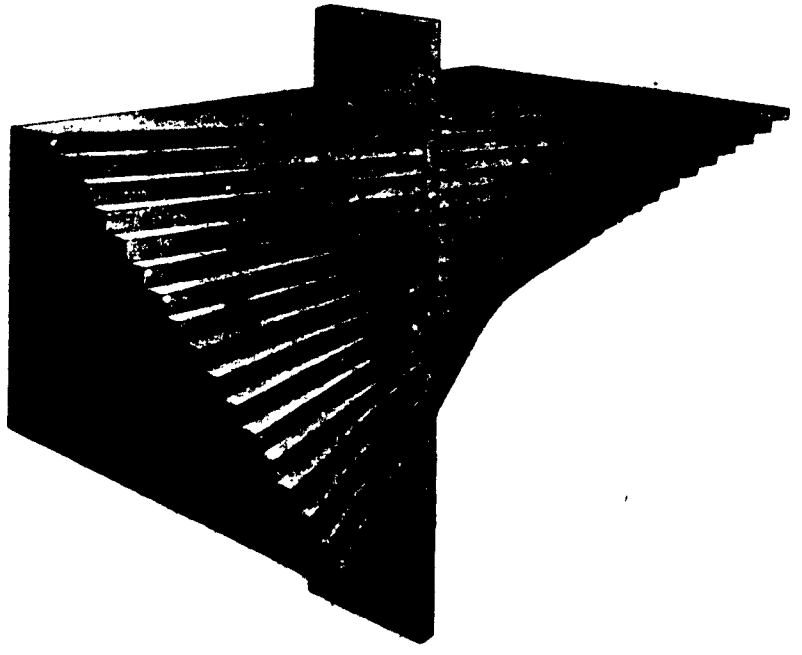

FIG. 3. A Mills Cross Transducer Configuration for One Directional Scanning.

*The Sperry sonar propagation and transducer computer was used for this computation.

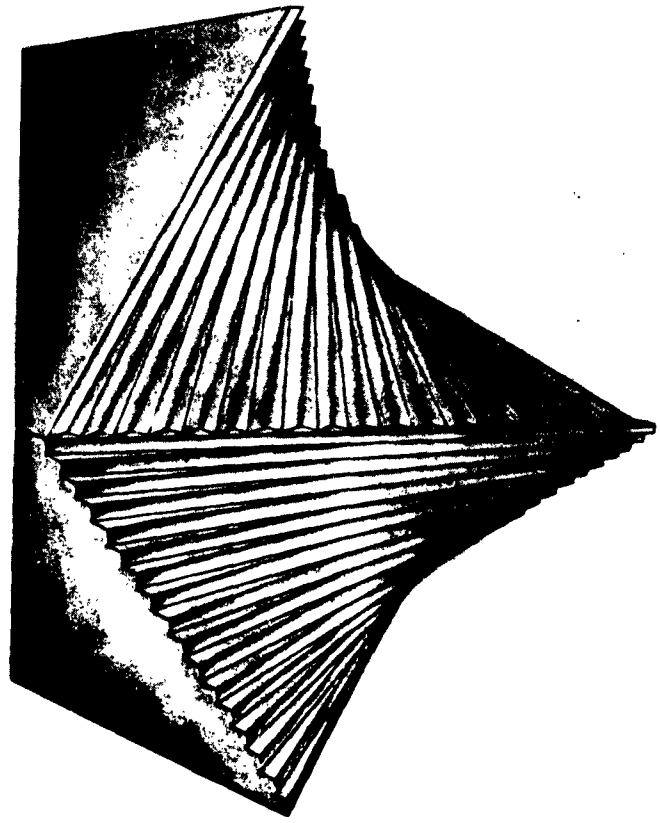

FIG. 4. A Mills Cross Transducer Configuration for Two Directional Scanning.

The one-directional scanning transducer has few problems other than those encountered with a conventional Mills cross. This transducer would have one element placed in a vertical position with several elements placed in horizontal positions at regular angles. This would allow the horizontal elements to be switched sequentially, parallel to the vertical transducer, to form several different Mills crosses, each pointing in a different direction, as shown in Sketch 10.

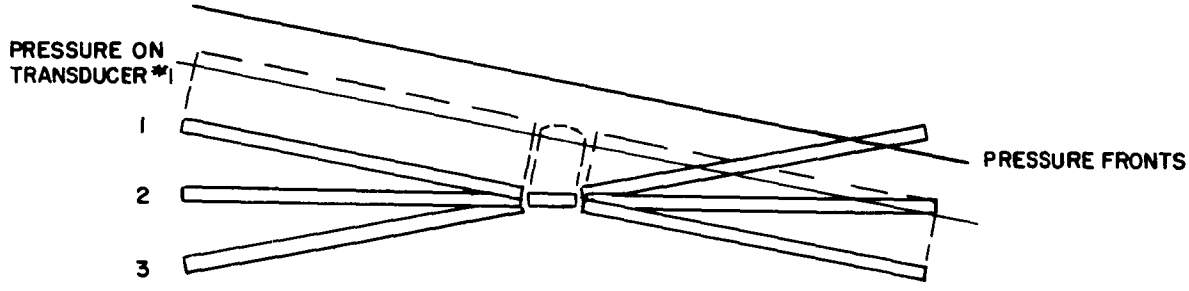

SKETCH 10

The combined signal produced by the vertical and #1 horizontal elements is lower because the vertical element is slightly twisted relative to the incoming signal. If it were desirable to switch through 20° with a signal fall-off of -3 db or less on the center transducer, this transducer would have to be 2.5 wavelengths or less in width. The side-lobe pattern is not apparently affected by the twisted vertical elements. However, a slight deterioration in quality might be expected in the areas of beam width and side lobes, especially when the configuration is a non-symmetrical cross. Construction problems, of course, increase with increased complexity of configuration. Each horizontal element should pass through the center of the vertical element and, if construction tolerances allow up to a 10-deg phase shift, this would be only 1/36 of a wavelength, or, for 1.5 Mc, a little over 0.001 inch. See Sketch 11.

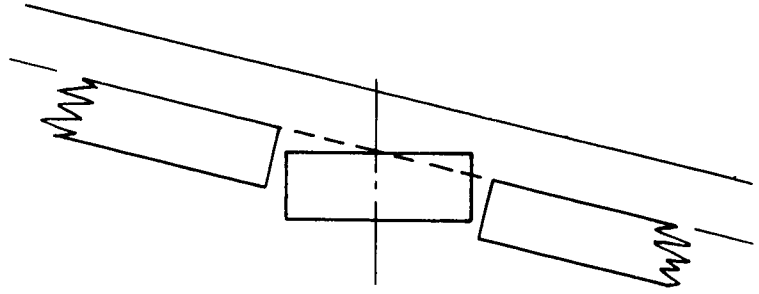

SKETCH 11

In a two-directional switching transducer it is probable that the horizontal and vertical groups of transducers might be separated a short distance, with a displacement for the worst condition being some multiple of $\lambda/2$. To examine the sensitivity pattern we will use a transducer element 200 wavelengths long and 200 wavelengths between centers (as shown in Sketch 12). At this point the signal would null out completely. Another unique point is demonstrated in Sketch 13 which shows the pressure waves again perpendicular to the plane of the drawing, resulting in maximum pressure on one transducer.

$$P_{av} = \Sigma P_{max}\ 1/2\ (1 + 0.636)$$

$$\frac{P_{av}}{P_{max}} = 0.818 = -1.7 \text{ db}$$

The same signal level will result at $(-\theta)$.

Another unique point is apparent on the sensitivity pattern when the plane of the pressure wave is maximum at the center of each transducer but passes through the point midway between this 1/4 wave separation. The pressure wave is not perpendicular to the plane of the paper and will be symmetrical on both transducer elements as shown in Sketch 14.

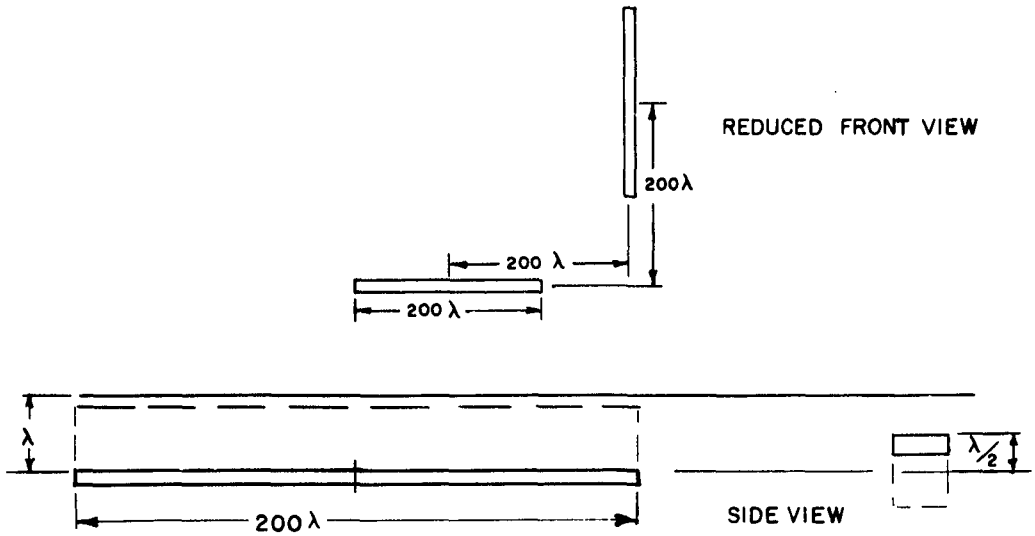

SKETCH 12

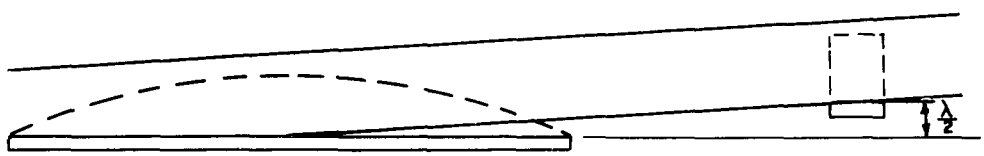

SKETCH 13

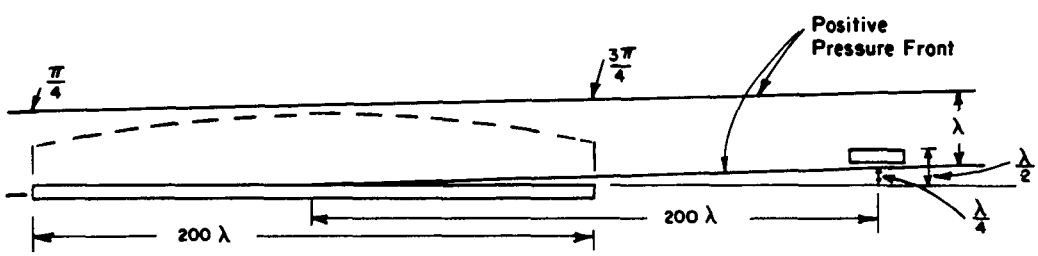

SKETCH 14

$$\frac{P_{av}}{P_{max}} = \int_{\frac{\pi}{4}}^{\frac{3\pi}{4}} \frac{w \sin x \, dx}{w \frac{\pi}{2}} \qquad w = \text{width} = 1$$

$$= \left| \frac{-\cos x}{\pi/2} \right|_{\frac{\pi}{4}}^{\frac{3\pi}{4}} = 0.903$$

$$= -0.9 \text{ db}$$

When the signal arrives well outside the normal beam width of either line transducer and in the beam of the other transducer, the signal level is down to the -6 db level--the same as for a standard Mills cross.

The results here are as one should expect: transducers with separations significant to their own dimensions have interference patterns within their own beam width. The results are further complicated with beam width and interference when the elements are not held in the same plane or in some parallel plane a multiple number of wavelengths away. These switching transducers, either one- or two-directional, could surely be constructed for special applications where a 6-decibel contrast is adequate.

ACOUSTICAL IMAGE TEST

Some tests have been conducted with a 1.5-Mc, 8-inch Mills cross transducer using directional mechanical scanning. The cross was constructed of round buttons which were shaded according to the Tschebyscheff distribution, Ref. 5, and mounted on a brass plate; cement thickness variation was 0.005 inches. One-eighth watt energy, transmitted from a single button about 38 feet away, covered the area of the target, which was a 4- x 4-ft Styrofoam board with lead weights, mounted on a lab stand at the deep end of a swimming pool. Figure 5 is a general view of the entire test setup showing the receiving and sending transducers close to the electronics. The inset in Fig. 5 is the acoustical image of the Styrofoam board; some return from a steel ladder also appears in the upper-left-hand corner. A complete description of the test, together with power loss calculations, appears in Appendix **A.**

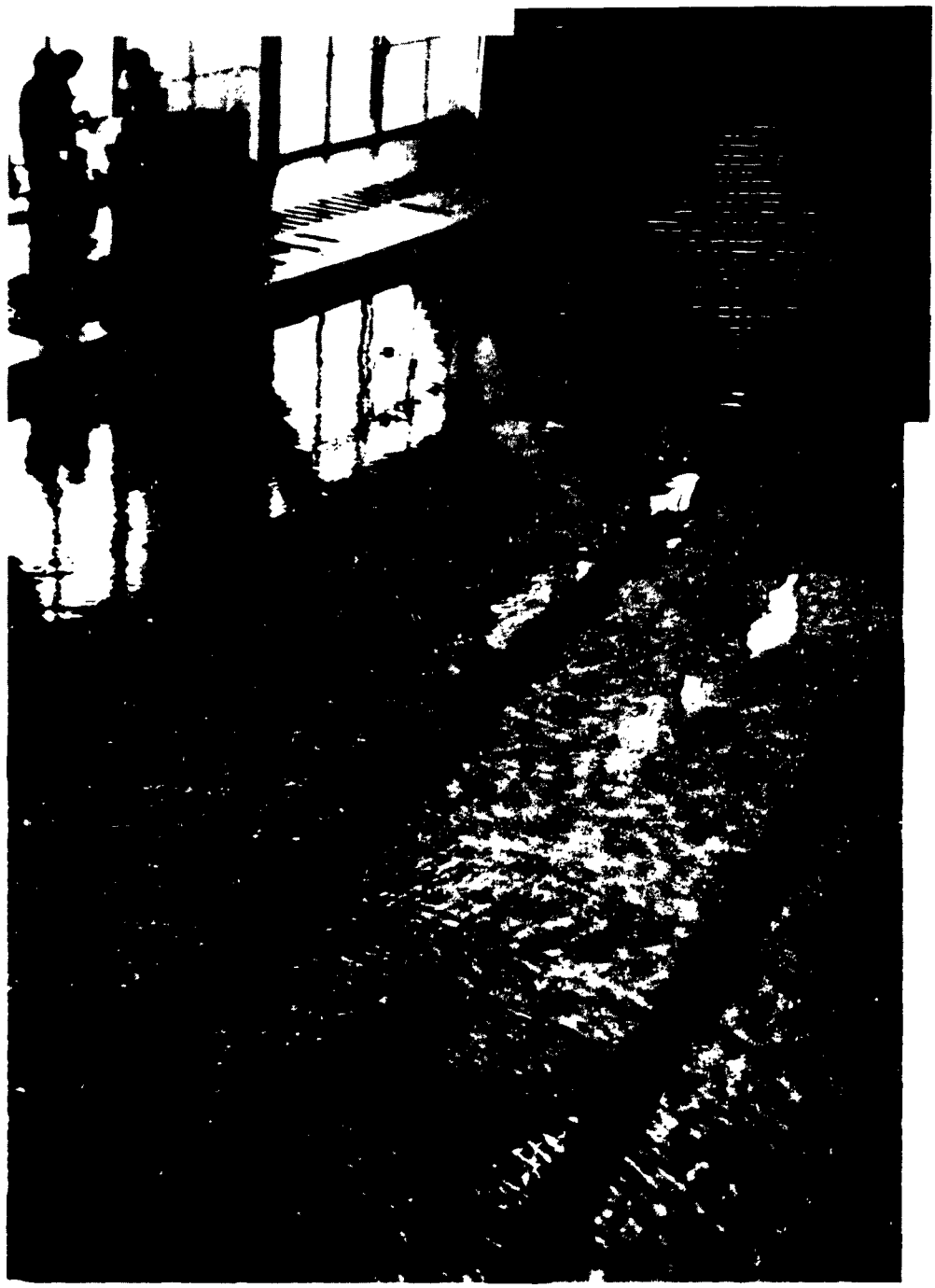

FIG. 5. Acoustical Test Setup in Swimming Pool;
(Inset) Image of Target From Acoustical Camera.

TRANSDUCER ACOUSTICAL IMPEDANCE MATCHING

The working mediums for transducer design must be impedance matched. The problem presented is similar to a transmission line problem. The receiving and transmitting transducers each present a separate problem since each one must be designed to have an impedance match to water. Since the energy emitted from the back of the transducer is not only wasted, but might also present a noise problem, the energy flow in this direction should be stopped. The normal reflected energy for thick reflectors is given by (Ref. 2, p. 110):

$$\frac{I_r}{I_i} = \frac{[(\rho c)_2 - (\rho c)_1]^2}{[(\rho c)_2 + (\rho c)_1]^2} = \frac{\left[1 - \frac{(\rho c)_1}{(\rho c)_2}\right]^2}{\left[1 + \frac{(\rho c)_1}{(\rho c)_2}\right]^2}$$

I_r = Intensity (reflected)

I_i = Intensity (incident)

By selecting a material with either a high or low ρc, most of the energy is reflected at the boundary. The high value acoustical impedance reflector reflects energy in phase; the low value acoustical impedance reflector reflects energy 180° out of phase. The phase of reflection and the resulting acoustical impedance at the reflected boundary determine the value of ρc. If a low ρc is chosen for the backing material such that

$$\frac{(\rho c)\ \text{backing}}{(\rho c)\ \text{transducer}} \cong 0$$

the energy from the back surface of the transducer is reflected and the transducer impedance is approximately matched to water.

The Smith Chart, Fig. 6, depicts the process and is ideal for use with nonabsorbent mediums. Although the transducer is an absorbent medium, the Smith chart can be used to understand the problem. Referring to the chart, move from the 0 impedance point clockwise around the chart one full revolution for every half wavelength on the exponential spiral inward (due to the lossy medium), Ref. 6. The spiral inward is probably too great to achieve the desired impedance match to water:

$$\frac{\rho c\ \text{water}}{\rho c\ \text{transducer}} = 0.05.$$

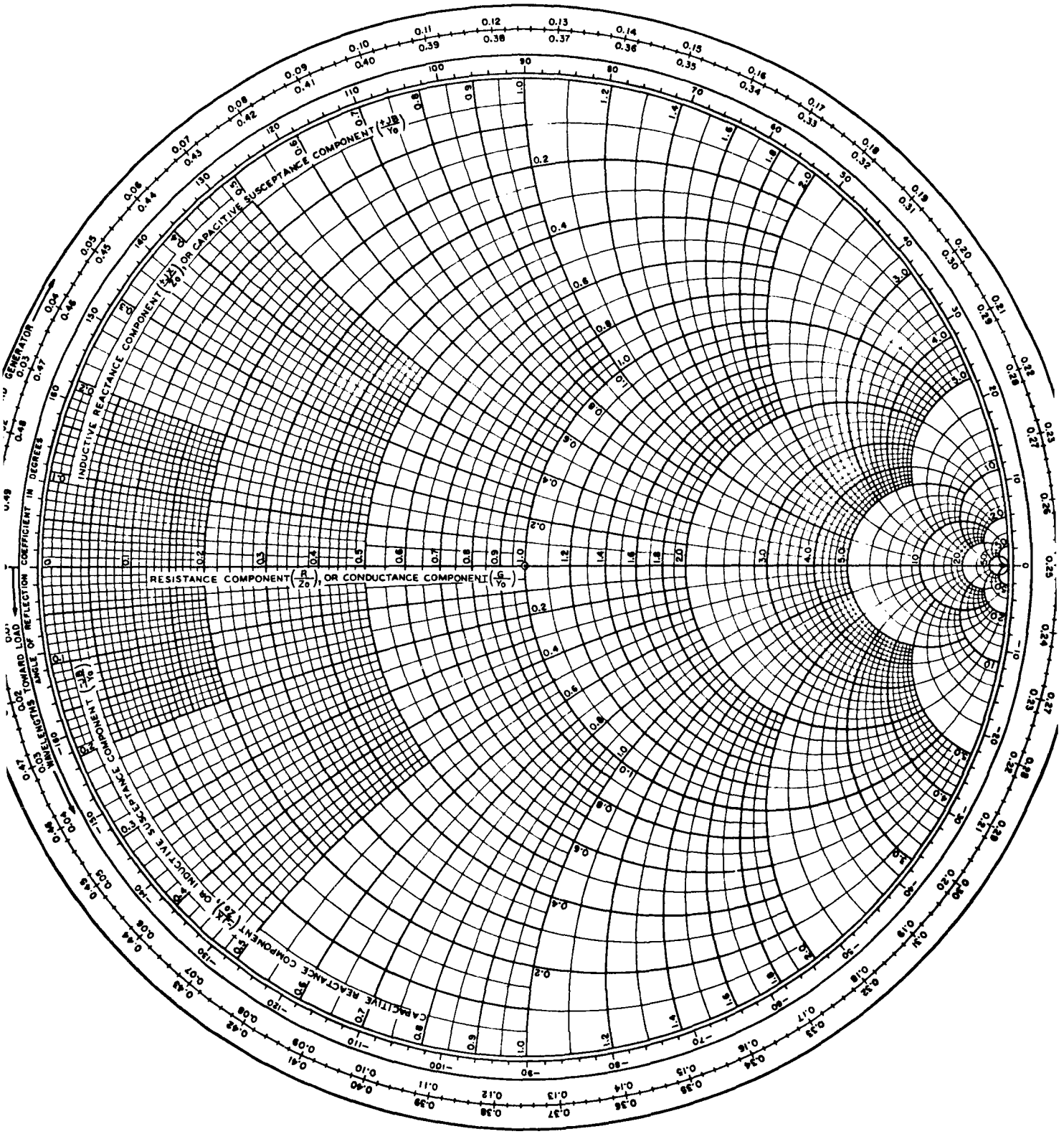

FIG. 6. Smith Chart.

If an acoustical impedance match is not achieved, a quarter wavelength matching plate of some material whose ρc is the geometric mean of the two impedances could be built on the transducer surface. As shown on the Smith Chart, the imaginary impedance implies a reflection other than a zero or 180-degree phase shift. This tends to shift the resonant frequency to a higher frequency if leading in phase--and to a lower frequency if lagging in phase.

LENS SYSTEMS

Increasing contrast over a Mills cross directional transducer would, apparently, require a circular configuration. A large circular transducer with mechanical scanning would not be desirable because of noise from turbulance; however, an acoustical-lens system with a matrix of receiving elements might possibly be used. For a circular area in such a system to have 0.25-degree resolution

$$\theta = \frac{1.22\lambda}{D}$$

$$D = 280\lambda$$

1.22 = a constant for circular configuration
θ = angular resolution, radians
λ = wavelength
D = diameter of lens

The definition for the resolution angle θ is one used in optics and involves resolution or separation of two points--i.e., when the center of the main lobe of each falls on the first null of the other (Raleigh's Criterion), Ref. 7. To determine the diameter of a transducer element, d, of a compatible 0.25-degree resolution system, if the focal length (f) equals 840 wavelengths (Sketch 15) where θ is the angle of minimum beam width due to the lens system

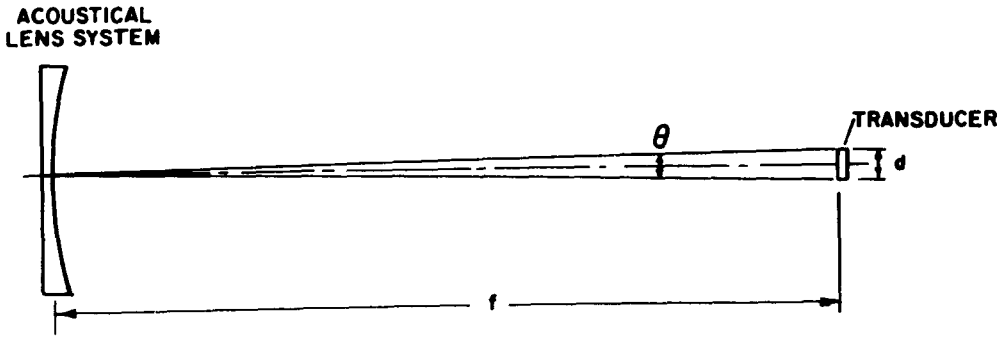

SKETCH 15

then

$$\theta = \frac{d}{f}$$

$$d = 840\lambda \ (0.25\text{-deg}) \ \frac{2\pi}{360} \ \frac{\text{rad}}{\text{deg}}$$

$$= 3.72\lambda .$$

Thus the receiving transducer button will have a diameter, d, of 3.7λ. The beam of this transducer is down 4 db at the aperture of the lens, Sketch 16.

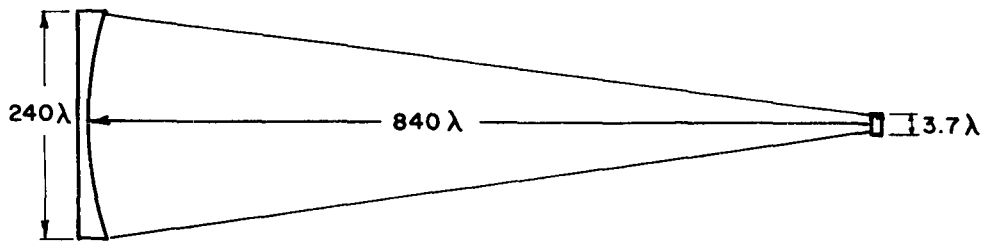

SKETCH 16

It is interesting that a given lens aperture and focal length always result in a transducer size compatible in resolution and beam width. It is probably better to use the angle of resolution for the lens as found on the Sperry sonar propagation and transducer computer to define the beam to one-half-power points so that both the lens and the receiving transducer are down to the one-half-power point at the edges. The resolution of the lens and button combination would, of course, be less for the two combined.

The Hopkins* formula, using resolving power (in a lens-emulsion system) as a function of certain image 'energy' diameters will probably apply. The formula:

$$R = 605 \ (d_e^2 + d_f^2)^{-1/2} ,$$

gives resolution R in lines/mm; d_e represents the diameter of the circle, which contains 30% of the image energy, and d_f is a constant of the emulsion. Both d_e and d_f are expressed in microns.

If we make $d_e = d_f$ then resolution is reduced from the limit of either one by the factor $(\sqrt{2})$. The equation gives reasonable results for this problem and it also shows the reduced resolution obtained with two limiting factors, d_e and d_f.

*Robert E. Hopkins, Rochester, N. Y.

Gain is the ratio of intensity (or the ratio of lens area to transducer area):

$$I_1 A_1 = I_2 A_2$$

and by definition

$$G = \frac{I_2}{I_1} = \frac{A_1}{A_2}$$

I_1 = intensity at lens

I_2 = intensity at transducer

A_1 = area of lens

A_2 = area of transducer

G = gain of lens

By reducing frequency, absorption is lowered and area is increased, resulting in increased power and reduced scan rate (this is an information theory limit). The scan rate upper limit requires one or more cycles of information before switching to the next element of the transducer matrix. In addition, the impedance of each transducer element would be reduced.

For $\theta = 0.25$ deg and F/3

$$G = \frac{A_1}{A_2} = \frac{\frac{\pi D_1^2}{4}}{\frac{\pi D_2^2}{4}} = \frac{D_1^2}{D_2^2}$$

D_1 = diameter of lens

D_2 = diameter of transducer

$$= \frac{(280\lambda)^2}{(3.7\lambda)^2} = 5.6 \times 10^3$$

$$= 37 \text{ db}$$

For a better comparison, the gain this method shows over the previously-discussed Mills cross system if both systems are at 1.5 Mc, is:

$$G = \frac{A_1}{A_2} = \frac{\frac{D^2}{4}}{1.35 \text{ cm}^2}$$

$D = 280\lambda = 11.2$ in.

$$= 38$$

$$= 16 \text{ db}$$

Both type and material of lens are germane. If a reflector type is selected, then steel gives 88% reflection efficiency, which can be even higher if a thickness of some odd multiple of one-quarter wavelength is used. Materials such as Monel, nickel, Inconel, molybdenum, and other rare metals (Ref. 3, p. 8) have a better reflection efficiency than steel.

For lens systems using membrane windows or thin reflecting surfaces the equation for thin plates should be used, Ref. 8.

The energy-transmission coefficient T_E and the energy reflection coefficient R_E for lossless thin plates and membranes of thickness d_p, and for normal incidence are given by:

$$T_E = 1 - R_E = \frac{1}{\left[1 + \frac{m^2 - 1}{2m}\right] \sin^2 \left(\frac{2\pi d_p}{\lambda_p}\right)}$$

d_p = thickness of plate

λ_p = a wavelength in the plate material

where

$$m = \frac{\rho_p c_p}{\rho_o c_o}$$

the relative acoustic impedance is the ratio of the acoustic impedance of the material to the acoustic impedance of the medium.

For the special case where

$$d_p \ll \frac{\lambda_p}{2}$$

d_p = thickness of thin plate
λ_p = wavelength in plate material

The equation reduces to

$$T_E = 1 - R_E \cong 1 - \left[\frac{(m)^2 - 1}{m} \pi \frac{d_p}{\lambda_p}\right]^2$$

For the relative acoustical impedance, very small values may be obtained. Thin plates of materials with very low acoustical impedance would make excellent reflectors.

For the reflected intensity of sound for a thick plate, the equation is:

$$R_E = \frac{P_r^2}{P_i^2} = \frac{I_r}{I_i} = \frac{[(\rho c)_2 \sin \theta_1 - (\rho c)_1 \sin \theta_2]^2}{[(\rho c)_2 \sin \theta_1 + (\rho c)_1 \sin \theta_2]^2}$$

In the case of the normal incidence:

$$R_E = \frac{P_r^2}{P_i^2} = \frac{[(\rho c)_2 - (\rho c)_1]^2}{[(\rho c)_2 + (\rho c)_1]^2}$$

θ_1 = angle of incidence

θ_2 = angle of transmission

R_E = energy reflection coefficient

P_r = power, reflected

P_i = power, incident

I_r = intensity, reflected

I_i = intensity, incident

P = density

c = speed of sound in media

1 = first medium

2 = second medium

If a refraction-type lens is used, it is desirable to have the acoustical impedance (ρc) of the two media equal. A difference of the velocity of sound, c, is required and absorption must be small. For a material like carbon tetrachloride, ρc is very close to water while c is about 2/3 that of water. A liquid-retaining window with 80% transmission would require a prohibitively thin containing membrane having a thickness of $d \cong \frac{\lambda}{60}$ for aluminum and $d \cong \frac{\lambda}{9}$ for Lucite. Perhaps half-wavelength material (sometimes called windows) could be used. It would not, however, be a perfect window between two materials having different acoustical impedances.

Other solid materials which might be used for lenses are Lucite, polystyrene, and polyethylene, which have a speed of sound greater than that of water. Of these materials, Lucite has a high c, (ρc), and absorption. In the case of polystyrene, the transmission of a single water-polystyrene boundary normal to the surface is 94% efficient--this fades to between 75 and 85% for reasonable acoustical-lens angles. The velocity of sound of polystyrene is about 1.5 times greater than that of water. Polyethylene has a density in the range of 0.95 and a c approximately 1.3 times greater than that of water. Polyethylene has a small impedance mismatch as the density is low and would make an excellent lens provided absorption characteristics are reasonable. Since these materials have speeds of sound greater than water, positive lenses would be concave and thus the absorption characteristics would amount to shading. Also, the transducer behind a lens element will be down to

about -3 db on the edges. This amounts to additional shading, which means the first side lobe should be greatly suppressed. Thus, the first side lobe is 180° out of phase and at -17.8 db on a circular element.

Unlike the photographic emulsions and some TV cameras where an increment of area also integrates this energy over time, the receiving transducer sums the signal over the area of the receiving element. In an acoustic problem, if lens quality is low (that is, if the pressure wavefront does not converge on the transducer in a uniform wavefront) the time of arrival is out of phase. As a result, standing waves form and energy cancellation occurs over the area of focus.

The shape of the sensitivity area of a transducer system (including reflecting and refracting lens systems with compatible transducers) is basically a function of the shape (aperture) of the energy-gathering surface. For example, a line transducer (long and narrow) can be shaded electrically by impedances, but the same thing can also be accomplished by narrowing the transducer at the ends as shown in Sketch 17.

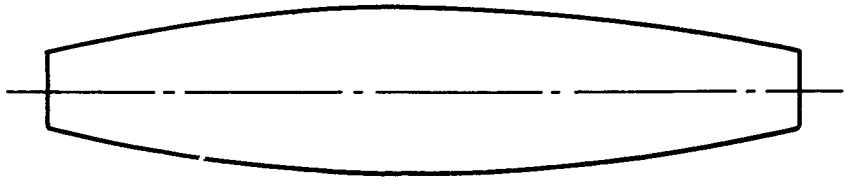

SKETCH 17

A lens with the same aperture shape would have the same pattern and, when combined with a compatible transducer, would have a wider beam by the factor of $\sqrt{2}$. The compatible transducer would be of the same general aperture shape, but would be mounted at crossed angles behind the lens.

LENS TESTS

Two acoustical lens systems tests were conducted to determine resolution and contrast of the system. The first test, using a 24-inch diameter, low-quality parabolic reflecting lens, resulted in standing waves in the area of focus. This was determined from the fact that the signal on a single receiving transducer (which sums the signal over the area of reception) would increase and then decrease when moved in small increments in any direction.

In the second and successful test a 5.75-inch aperture glass parabolic mirror (the 0.66 glass-to-water reflection coefficient is adequate

for these tests) with a focal length of 24 inches was used to view a 3/8-inch button located 84 inches from the lens. The resulting image distance from the lens was approximately 34 inches. Several 3 x 3 receiving matrix configurations were used; however only one was fully successful.

Two construction factors are believed to have made the difference between the successful and unsuccessful tests. In the successful test, the back-conducting surfaces were cemented to a very thin conducting aluminum foil, then backed with a foam plastic. This accomplished better acoustical matching and reduced the possibility of shear waves in the backing-material transferring energy. The unsuccessful matrices had thicker foil and micarta backing from one crystal to another. Also in the second test, extra care was used on the front surface connection to reduce matrix solder and wire mass and thus maintain the resonant frequency of the piezoelectric transducer and the impedance match to water. Sketch 18 shows the transducer arrangement--the circles indicate the signal strength of the beam over the area of the transducer.

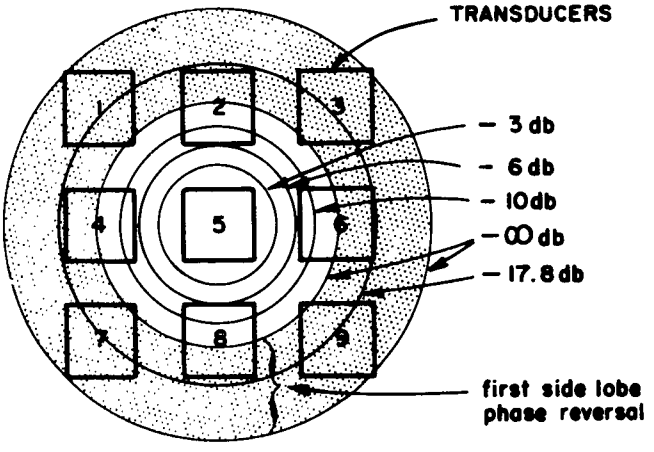

SKETCH 18

The signal levels of each transducer were compared to the center one (which was estimated at -1 db from the maximum level). These levels for transducers 2, 4, 6, and 8 were -12 to -16 db; for corner transducers 1, 3, and 9 the signal strength was nearly zero; while corner transducer 7 had a -14 db reading.

To simulate close spacing, the beam was moved to one crystal width from the center of the No. 6 crystal in a setup as shown in Sketch 19, to determine the signal strength on that crystal. The resulting signal was about -6 db. Optical alignment and focus were used to determine beam center location focus. It was also determined during the test that focus could be accomplished by observing the acoustical signal levels.

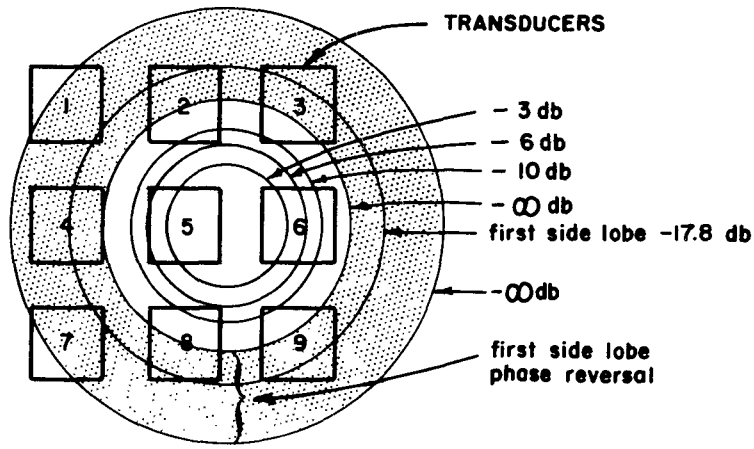

SKETCH 19

AMPLIFYING AND SWITCHING

Since it is desirable to receive minimum signal levels, which would of necessity be greater than thermal noise levels (see Appendix B), high-gain amplifiers are indicated. However, a large matrix transducer array involves so many transducer elements that the individual preamplifiers on each element might be prohibitive in cost for many applications. There is the possibility of direct switching at the 10 to 100 μvolt level for small piezoelectric transducers. That is, a 0 to +20 db level, referenced to 1 microbar would be obtained when the calculated impedance of the transducer is 1,000 ohms and the transducer is not greater than 0.2 cm^2 in area. (See Appendix C for switching technique studies.)

Ultrasonic imaging tubes would be a reasonable solution for the high-speed, low-level switching problem if these tubes had high sensitivity. Although none is available at this time, the General Electrodynamics Corporation and the TE Company have proposed development of a vidicon-type, acoustical-imaging tube having a 10 to 100 μvolt sensitivity, or a signal level of +60 to +80 db.

CONCLUSIONS

As a result of this study it is concluded that an acoustic-picture device, consistent with theoretical and technical limits, can be built. Such a device would probably use a lens system with electronic switching on a matrix array of transducers or a large round transducer with mechanical scan.

It is indicated that reasonable conservative values for an acoustical source might be:

Signal strength transmitted	+115 db
Signal strength received	0 db*
Target loss	-15 db
which leaves about for spreading & losses.	100 db

Range of the system could be 150 ft at 1.5 Mc, 200 ft at 1 Mc, or 850 ft at 100 kc. This range and other greater ranges could be accomplished by using low frequencies which have low absorption coefficients. However, they would require large transducer systems to gather in low-signal levels and would have poor resolution.

A practical upper limit in range is a function of object size, or minimum resolution and maximum permissible transducer size. For example, a two-mile system allowing 100-db loss due to spreading and absorption, would require a frequency of 30 kc or less. A ten-foot diameter system would have a 1.0-deg beamwidth at two miles, thus limiting identification to comparatively large objects.

Since there are compromises within resolution, framing rate, and distance of coverage, etc., a general-purpose instrument is not practical. However, systems could be tailored for specific instrumentation purposes. For example, several line transducers or equivalent lens systems could be arranged for sky-screen affect or they could be grouped at a single location for angle data, with the possibility of obtaining range from the time delay of the return signal. Although the conventional Mills cross does not have enough contrast for this application a two-way switching Mills cross could be used for angle determination. The two arrays would probably be monitored separately for this use.

---

*0 db is referenced to one μb of pressure.

Appendix A

ACOUSTICAL IMAGE TESTS

Underwater acoustical imaging tests were conducted in the Station swimming pool using an experimental transistor transmitter and receiver, operating at 1.5 Mc. The transmitter controlled both the pulse length and the duration between pulses; the receiver had blanking during transmission.

A single barium titanate transducer, transmitting at 1/8 watt, and an unmodified 8-inch, 1.5-Mc Mills cross constructed of rounded buttons and shaded according to the Techebyscheff distribution, were mounted on a brass plate. (This brass plate lowered the acoustical transfer efficiency and was found to be one of the worst possible materials for acoustical impedance matching.) The receiving transducer head was mounted in a two-axis yoke with azimuth motor drive and an elevation-stepping relay using potentiometers for both position determinations. The potentiometers were used to control the position of the beam on the oscilloscope. Signal-return information was used to modulate the beam intensity. The target was a weighted 4-ft square Styrofoam board mounted on a Lab stand at the deep end of the swimming pool. The concrete pool sides were highly-efficient reflectors so the test was set up diagonally in the pool. Directly behind the target was an outlet of a turbine-pump recirculation system that created bubbles. These bubbles were sufficient to give returns. Figure 7 shows the return from air bubbles directly behind and above the target and a distorted reflection of the target off the curved bottom. Figure 5, page 19, shows the test setup and the target return. Here there was very little return from the bubbles and the scan was not low enough to get bottom reflections.

Pulse-length investigation was made with a circuitry which would not fully respond to the short pulses. However, by gating the receiver ON, it was determined that two cycles of information would be sufficient to ascertain a return from one point on the target.

During the continuous transmission investigation phase the return signal, which came off the side of the pool 30 feet away, was compared with the background signal level. When the receiving transducer was about two feet to the side of the transmitting transducer, and shielded from it, the return signal indicated 14 units on an oscilloscope while the background level was 5 to 9 units. This is essentially a 0 background level for continuous transmission. There does not appear to be a high enough signal-to-background level for an effective continuous transmission system.

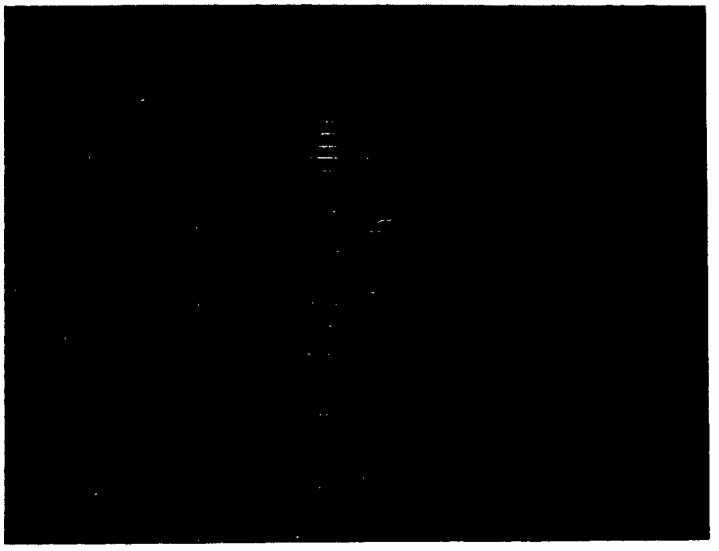

FIG. 7. Acoustical Image of Target Showing Reflection and Air Bubbles.

A study of the present system was next undertaken in order to verify previous power calculations. The transmitting transducer had a diameter of 3/8 inch (0.952 cm), and a transmitting area of 0.714 cm^2. The beamwidth to the 1/2 power points was 6.4 deg with the power assumed to be spreading uniformly over this solid angle. A target was placed 27 feet (8.25 meters) from the transducer as shown in Sketch 20. If the near field effects are projected horizontally they will cross the solid angle at a distance of 8.65 cm.

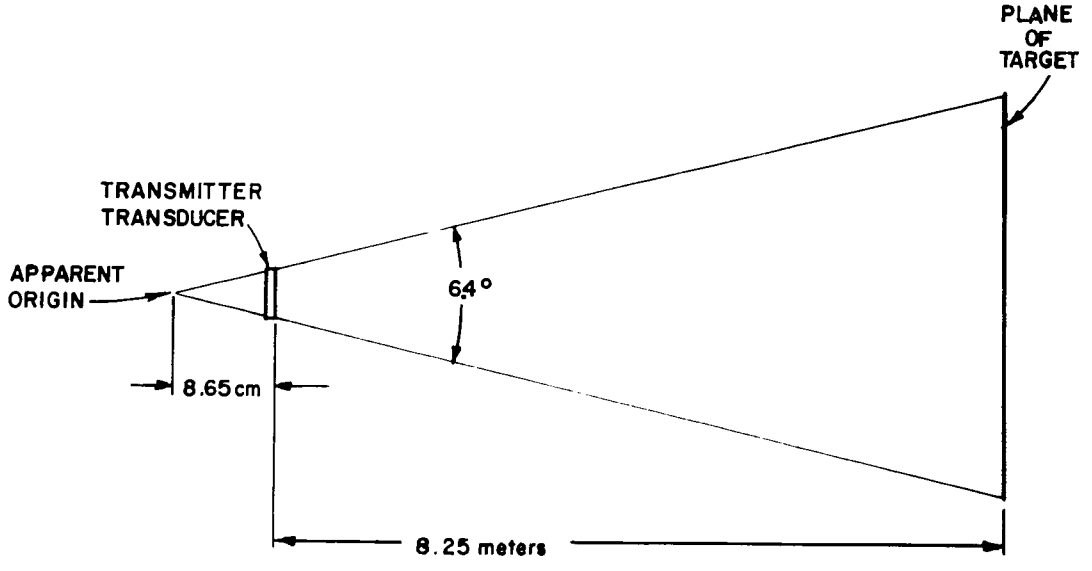

SKETCH 20

The transmitted power was 10 volts peak-to-peak across the 100-ohm transducer. Thus the RMS voltage is:

$$V_{RMS} = \frac{10\ v}{2\sqrt{2}} = 3.58\ v$$

The RMS power is:

$$\text{Power} = \frac{(3.58\ v)^2}{100\ \Omega} = 0.125\ \text{watts}$$

The power radiated per unit area of transmitting surface.

$$\frac{\text{Power}}{\text{Area}} = \frac{0.125\ \text{watts}}{0.714\ \text{cm}^2} = 0.175\ \frac{\text{watts}}{\text{cm}^2}$$

The barium titanate transducer has a mechanical-to-electrical efficiency of 30 to 40% and a surface-to-water transmission of 30%. (This might be even lower if the transducers (which for this test were mounted on a brass plate that increased the acoustical impedance mismatch) were mounted on a plate constructed of a more favorable material.) Using the above values, acoustic power intensity delivered to the water is:

$$I = 0.30 \times 0.30 \times \frac{\text{Power}}{\text{Area}} = 0.09 \times 0.175 = 0.016\ \frac{\text{watts}}{\text{cm}^2}$$

The RMS pressure (P) transmitted through this acoustic power is:

$$P = \sqrt{\rho c\ I \times 10^7}$$

P = pressure average $(\frac{\text{dyne}}{\text{cm}^2})$

ρc = acoustic impedance (acoustic ohms)

I = acoustic intensity $(\frac{\text{watts}}{\text{cm}^2})$

$$P = \sqrt{154{,}000 \times 1.6 \times 10^5}$$

$$= 1.57 \times 10^5\ \frac{\text{dynes}}{\text{cm}^2}$$

$$P = 20 \log 1.57 \times 10^5\ \text{db}$$

$$= 104\ \text{db referenced to 1}\ \frac{\text{dyne}}{\text{cm}^2}\ \text{or 1 microbar.}$$

The spreading loss varies by the square of the distance from the origin. Since the energy had to travel to the target and back to the receiver the distance is 16.5 meters. Therefore,

$$\text{Spreading loss} = \left(\frac{16.5 \text{ meters}}{8.65 \text{ cm}}\right)^2 = 3.87 \times 10^4$$

$$\text{Spreading loss in db} = 10 \log 3.87 \times 10^4 = 46 \text{ db.}$$

This 16.5-meter round trip distance from transmitter to target to receiver is approximately 18 yd. The water absorption of sound at 1.5 Mc is 0.70 db/yd, so:

$$\text{Absorption loss} = 0.70 \frac{\text{db}}{\text{yd}} \times 18 \text{ yd}$$

$$= 12.6 \text{ db}$$

The last loss to consider is target loss. The target of Styrofoam ($4 \frac{\text{lb}}{\text{ft}^2}$ density) can be considered similar to air for purposes of calculations. The amount of reflected energy, R, from the target is:

$$R = \frac{Z_1 - Z_2}{Z_1 + Z_2}$$

$Z = \rho c$ = acoustic impedance

ρc for air = 42 dyne cm^3

ρc for water = 150,000 dyne cm^3.

$R \cong 1$

Since the target surface was rougher than a wavelength, reflection spreading was greater than allowed for under spreading loss, which assumed mirror-like reflections.

The received signal is fed directly from the transducer into a high-impedance amplifier. The effective transducer impedance, with all of the parallel buttons and shading resistors, is 3.37 Ω. Since the receiver has an input impedance of about 1,000 Ω, then each button was probably not loaded down. The voltage out of the receiving transducer is 40 μvolts (estimated from the output voltage of the receiver) and is also the voltage across one button. The power out of one receiving button will be:

$$\text{Power} = \frac{E^2}{R} = \frac{(40 \times 10^{-6} \text{ v})^2}{100}$$

$$= 16 \times 10^{-12} \text{ watts/button}$$

$$I = \frac{16 \times 10^{-12} \text{ watts}}{0.714 \text{ cm}^2}$$

$$= 22.5 \times 10^{-12} \frac{\text{watts}}{\text{cm}^2}$$

Assuming a 30% mechanical-to-electrical efficiency and a 30% transfer of energy between water and the transducer surface

$$I = 0.30 \times 0.30 \times I_{water}$$

$$I_{water} = \frac{1}{.09} \times 22.5 \times 10^{-12} \frac{\text{watts}}{\text{cm}^2} = 248 \times 10^{-12} \frac{\text{watts}}{\text{cm}^2}$$

$$P = \sqrt{154{,}000 \times 248 \times 10^{-12} \times 10^{7}}$$

$$= 20 \frac{\text{dynes}}{\text{cm}^2}$$

The power in db's is:

$$P = 20 \log 20 = 26 \text{ db}$$

Summing the above calculated losses we have 46 db spreading loss, 13 db absorption loss, and virtually no target loss. The estimated return level at the receiver should be:

104 db - 46 db - 13 db = 45 db.

The calculated value of the received signal is 26 db, thus we have 19 db of unaccounted signal loss. The summation of losses assumes a perfect target reflector, but this may not be the case. We first assumed a flat target, but due to water currents set up by the continuous flow of water through the pool's filters, the target was bent into a slightly convex surface. This would account for more spreading of the reflected signal, thus greater spreading losses. It also became impossible to set the target up so that it would be perpendicular to the beam, therefore the returned beam was not reflected directly toward the receiver. In addition, it is important to note that the Styrofoam surface was rough compared to one wavelength, which would cause scattering of the reflected energy. This probable cause of the added target losses is confirmed by the fact that much stronger returns were recorded from the sides of the pool when they were normal to the beam.

Appendix B
MINIMUM THERMAL NOISE

The minimum thermal noise level which could be expected in an amplifier or switching circuit for an acoustic lens device is shown below. For these calculations, the switching rate between crystals was 500 kc, thus making the bandpass (Δf) of the amplifiers at least 500 kc.

$$E^2_{noise} = 4RkT\Delta f$$

E = RMS thermal voltage

R = resistance of element = 1000Ω

k = Boltzmann constant = $1.38 \times 10^{-23} \frac{\text{joules}}{^\circ\text{K}}$

T = Temperature in degrees Kelvin = 288°K

Δf = bandpass = 500 kc

$$E^2 = \left[4 \times 1000 \text{ ohms} \times \frac{\text{v-sec}}{\text{coulomb-ohm}} \times 1.38 \times 10^{-23} \frac{\text{joule}}{^\circ\text{K}} \times \frac{\text{v-coulomb}}{\text{joule}}\right] \left[288^\circ\text{K} \times 500 \times 10^3 \frac{\text{cy}}{\text{sec}}\right]$$

$$E^2 = 8.0 \times 10^{-12}$$

$$E = 2.8 \times 10^{-6} \text{ volts} = 2.8 \text{ microvolts}$$

Noise power is calculated:

$$P_N = \frac{E^2}{R} = \frac{8.0 \times 10^{-12}}{10^3}$$

$$P_N = 8 \times 10^{-15} \text{ watts}$$

$$P_{db} = 10 \log \frac{P_N}{10^{-3} \text{ watts}} = 10 \ (-12.9) \text{ dbm}$$

$$P_{noise} = -129 \text{ dbm}$$

There is also a possibility of using several parallel channels of amplification, each channel switching through a different section of crystals. Since each amplifier would now have fewer crystals to switch, the switching rate could be reduced by the same factor as there are channels of amplification. Thus 10 channels would reduce the rate of switching to 50 kc. The noise voltage (E) now would be 0.9 microvolts and the noise power would be -139 dbm. The signal-to-thermal-noise ratio could therefore be reduced by increasing the number of channels of amplification.

Appendix C

HIGH FREQUENCY COMMUTATING

During the initial development of an underwater acoustic-imaging device, a need arose for a high-speed switching circuit capable of commutating over 1,000 channels of μvolt signals at a 500 kc rate. The switching circuits had to be low in cost/channel due to the large number of channels required. On the basis of cost/channel, two devices were considered: Burroughs beam-switching tubes (since they would commutate with pulses from a single flip-flop), and diodes (since they were comparatively inexpensive). Considering these two devices, three circuits were evaluated.

Before establishing circuits, switch requirements were considered. Each switch was to be connected to a barium-titanate transducer which had an a-c impedance to water of about 1,000 ohms at 1.5 Mc, and a d-c impedance of 5,000 ohms. The switching circuit had to commutate these 1,000 transducers by detecting 1.5 Mc signals with amplitudes between 10 and 100 μvolts. These signals could then be fed into a single amplifier for detection and display.

The first switching device considered was the Burroughs beam-switching tube. This tube seemed applicable since only a flip-flop type circuit was needed to drive it. With proper circuitry, the tubes would switch through 10 channels, then pulse the next tube ON. Thus, with a minimum of external circuitry, the tubes would be able to commutate a large number of channels.

The BD301 tube was used in this case because of its availability, but for future transistor circuits the BD308 tube should be used. The 1.5-Mc signal was fed into the spade grid of the tube; in turn this signal modulated the target voltage in such a way that the target's output showed a slight amplification. The targets of each channel were then fed into a single amplifier through diodes so that the on-target voltage would not affect the other targets. The driving circuit could be a single multivibrator with one plate going to the 0 grid and the other plate to the No. 1 grid.

The following circuit, Sketch 21, was used to prove this technique:

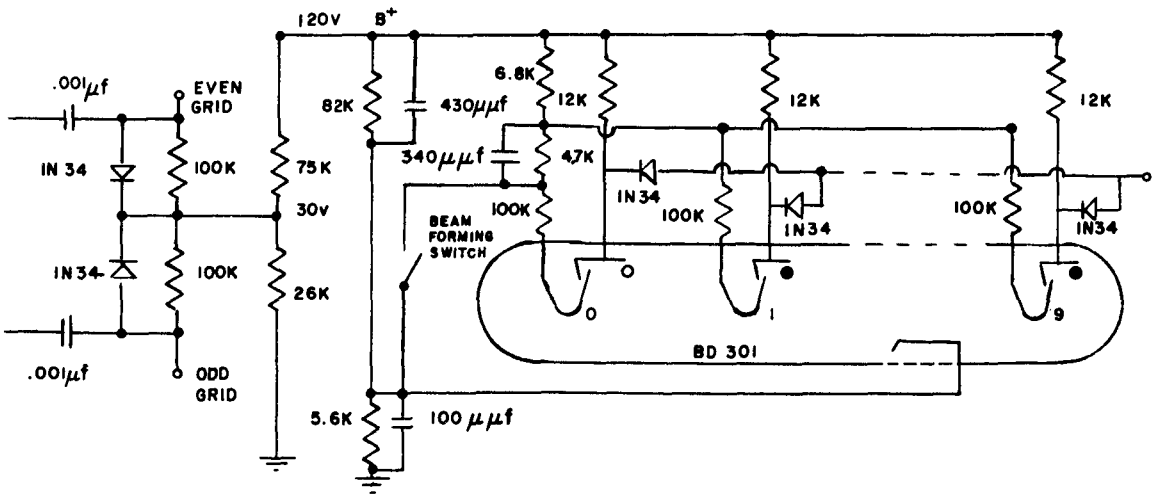

SKETCH 21

The circuit shown was able to commutate through 10 channels of one tube at a 500-kc rate; however, the tube was very noisy. Switching spikes in the order of 10 volts were noted and a tube thermal-noise level of near 10 millivolts kept smaller input signals from being seen. It would be possible to blank the switching spike in the amplifier but the tube noise seemed too intense for the small signals being considered.

The next circuit attempted, Sketch 22, used a simple diode-switching arrangement.

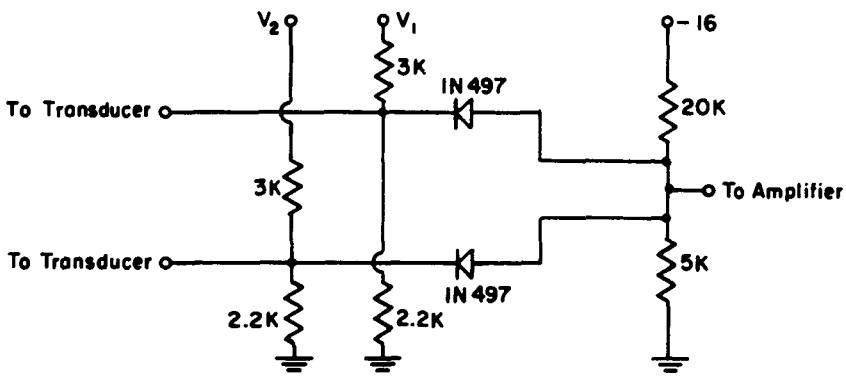

SKETCH 22

Applying a voltage at V_1 causes the diode to be forward biased and thus allows the 1.5-Mc signals to pass. Since the other diodes are reverse-biased, they do not load the next circuit.

Switching noise using diodes was not as severe as with beam-switching tubes. Spikes could be kept down to less than 0.05 volts and channel noise was less than 50 μvolts peak-to-peak for average peak levels. This circuit seemed to work satisfactorily except for signal strength variations due to diode thermal characteristics.

In order to commutate a large group of such switches, it would be possible to connect the point V_1 of each switch in a matrix fashion, as shown in Sketch 23.

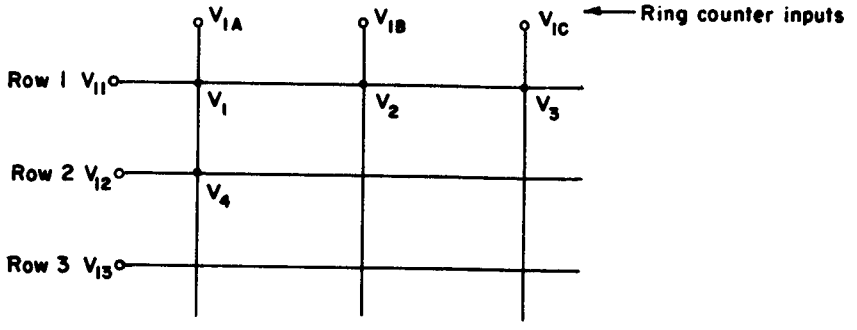

SKETCH 23

Using a ring counter, one-half the voltage necessary to turn on the diodes could be supplied in turn to each row and column. That is, Switch #1 could be turned on with voltages applied to Row #1, Column #1. Using a 500-kc ring counter for the columns allows the first row to be switched. By applying voltages to the rows with a slower ring counter, each column could be switched in Row #1, then, switching rows, the column in Row #2 could be switched, etc. Thus, only two ring counters with 32 channels each need be used for switching the diodes.

The third circuit, Sketch 24, is very similar to the previous diode switch except for the method of coupling it to the transducer. By using transformer coupling, a voltage stepup would be possible. The tuned circuit would have to have a bandwidth of greater than 500 kc, which is the switching rate. However, this circuit was plagued by ringing, apparently caused by switching transients. However, very little study was given to this particular problem.

After the 1.5-Mc signal passes through the switch, it must be amplified. A broad band amplifier was tried as a quick solution to the problem. One stage of this circuit is shown in Sketch 25.

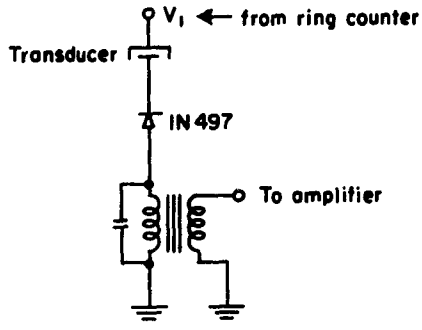

SKETCH 24

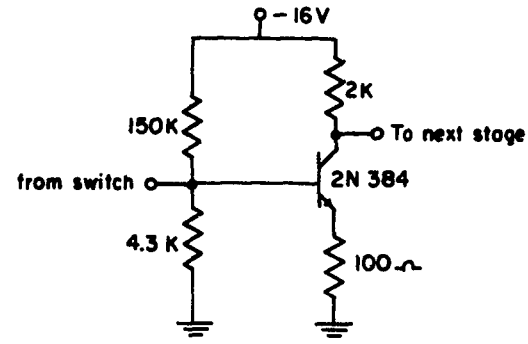

SKETCH 25

The input to each amplifier stage was biased so as to allow the signal to pass while clipping off the switching spike. This was continued until a 100-μvolt RMS signal produced a 5 volt output. At this point thermal problems became a predominant factor. A small change in diode current due to thermal effects would cause the switching spike to vary in amplitude some 100 μvolts, thus shifting the average signal level of the last amplifier so that it would clip the signal rather than the spike. It would appear that with some proper temperature-compensating networks a more constant gain could be obtained, thus preserving the signal.

Tests to date indicate that a satisfactory switching technique can be found. So far, 1.5-Mc signals at levels of less than 100-μvolts RMS have been commutated at a rate near 400 kc. These signals were then amplified to about 5 volts RMS. Careful diode selection and temperature-compensation circuits in the amplifier would definitely improve the present design.

REFERENCES

1. Hershberger, W. D. Principles of Communication Systems. New York, Prentice-Hall, 1955. P. 46.

2. Horton, J. W. Fundamentals of Sonar. Annapolis, Md., U. S. Naval Institute, 1957. Pp. 37, 49.

3. U. S. Naval Ordnance Laboratory. An Evaluation of Image Techniques in the Ultrasonic Inspection of Material, by W. R. Turner. Silver Spring, Md., NOL/WO, 2 July 1956. (NAVORD Report 4090). P. 10.

4. American Institute of Physics Handbook, coordinating editor, Dwight E. Gray. New York, McGraw-Hill, 1957. Section 3, p. 71.

5. Naval Ordnance Laboratory, Corona. Tschebyscheff Antenna Distribution, Beamwidth, and Gain Tables, by Lawrence B. Brown and Glenn A. Scharp. Corona, Calif., NOLC, 28 February 1958. (NAVORD Report 4629, NOLC Report 383).

6. Bronwell, Arthur B. and Robert E. Beam. Theory and Application of Microwaves, 1st ed. New York, McGraw-Hill, 1947. Pp. 170-1.

7. Jenkins, Francis A. and Harvey E. White. Fundamentals of Physical Optics, 3rd ed. New York, McGraw-Hill, 1957. P. 300.

8. Hueter, Theodor F. and Richard H. Bolt. Sonics. New York, John Wiley & Sons, 1955. P. 260.

Negative Numbers of Illustrations

Frontispiece.	LHL LO 70513
Fig. 1.	none
Fig. 2.	none
Fig. 3.	LHL LO 63777
Fig. 4.	LHL LO 63778
Fig. 5.	LHL LO 62585
Fig. 6.	none
Fig. 7.	none

INITIAL DISTRIBUTION

11 Chief, Bureau of Naval Weapons
- DLI-31 (2)
- FF (1)
- R-362 (1)
- RM-2 (1)
- RMGA-41 (1)
- RMWC-521 (1)
- RMWC-533 (1)
- RRRE-3 (1)
- RTSA-21 (1)
- Steering Committee Member, IRIG (1)

2 Chief of Naval Research
- Member Meteorological Working Group, IRIG (1)
- Code 104 (1)

2 Naval Air Development Center, Johnsville

1 Naval Air Test Center, Patuxent River (Aeronautical Publications Library)

5 Naval Missile Center, Point Mugu
- Steering Committee Member, IRIG (1)
- Member, Electromagnetic Propagation Working Group, IRIG (1)
- Members, Optical Systems Working Group, IRIG (2)
- Technical Library (1)

1 Naval Ordnance Laboratory, White Oak (Library)

1 Naval Ordnance Missile Test Facility, White Sands Proving Ground (Technical Library)

1 Naval Postgraduate School, Monterey

1 Naval Research Laboratory (Code 2021, H. P. Birmingham)

1 Naval Station, Roosevelt Roads, Puerto Rico

1 Naval Weapons Laboratory, Dahlgren (Technical Library)

2 Naval Weapons Services Office

2 Navy Electronics Laboratory, San Diego
- D. C. Jensen (1)
- Dr. M. Lund (1)

1 Chief of Ordnance (Steering Committee Member, IRIG)

1 Aberdeen Proving Ground (Ballistic Research Laboratories)

6 Redstone Arsenal
- Members, Optical Systems Working Group, IRIG (2)
- Technical Library, ORDXR-OTL (4)

1 Signal Corps Engineering Laboratories, Fort Monmouth (Technical Document Center)

9 White Sands Missile Range
- Secretariat, IRIG (1)
- Steering Committee Member, IRIG (1)
- Member, Electromagnetic Propagation Working Group, IRIG (2)
- Members, Optical Systems Working Group, IRIG (2)
- Technical Library (3)

ABSTRACT CARD

U. S. Naval Ordnance Test Station
A Study of Underwater Acoustical Imaging, by E. E. Curry. China Lake, Calif., NOTS, November 1962. 42 pp. (NAVWEPS Report 7889, NOTS TP 2882), UNCLASSIFIED.

ABSTRACT. TV-like pictures, showing position and shape of underwater missile test items are obtained by using a directional-scanning sonar method. This report is a systems study made to investigate the problems of acoustical imaging within the broad concept of such an instrumentation device. It covers

(Over)
1 card, 4 copies

U. S. Naval Ordnance Test Station
A Study of Underwater Acoustical Imaging, by E. E. Curry. China Lake, Calif., NOTS, November 1962. 42 pp. (NAVWEPS Report 7889, NOTS TP 2882), UNCLASSIFIED.

ABSTRACT. TV-like pictures, showing position and shape of underwater missile test items are obtained by using a directional-scanning sonar method. This report is a systems study made to investigate the problems of acoustical imaging within the broad concept of such an instrumentation device. It covers

(Over)
1 card, 4 copies

U. S. Naval Ordnance Test Station
A Study of Underwater Acoustical Imaging, by E. E. Curry. China Lake, Calif., NOTS, November 1962. 42 pp. (NAVWEPS Report 7889, NOTS TP 2882), UNCLASSIFIED.

ABSTRACT. TV-like pictures, showing position and shape of underwater missile test items are obtained by using a directional-scanning sonar method. This report is a systems study made to investigate the problems of acoustical imaging within the broad concept of such an instrumentation device. It covers

(Over)
1 card, 4 copies

U. S. Naval Ordnance Test Station
A Study of Underwater Acoustical Imaging, by E. E. Curry. China Lake, Calif., NOTS, November 1962. 42 pp. (NAVWEPS Report 7889, NOTS TP 2882), UNCLASSIFIED.

ABSTRACT. TV-like pictures, showing position and shape of underwater missile test items are obtained by using a directional-scanning sonar method. This report is a systems study made to investigate the problems of acoustical imaging within the broad concept of such an instrumentation device. It covers

(Over)
1 card, 4 copies

NAVWEPS Report 7889

the interrelationship of absorption, bandwidth, information-theory limits, and beam theory for transducers and acoustical lenses.

NAVWEPS Report 7889

the interrelationship of absorption, bandwidth, information-theory limits, and beam theory for transducers and acoustical lenses.

NAVWEPS Report 7889

the interrelationship of absorption, bandwidth, information-theory limits, and beam theory for transducers and acoustical lenses.

NAVWEPS Report 7889

the interrelationship of absorption, bandwidth, information-theory limits, and beam theory for transducers and acoustical lenses.

1 Headquarters, U. S. Air Force (Steering Committee Member, IRIG)
1 Air Force Systems Command, Andrews Air Force Base
(Steering Committee Member, IRIG)
1 Tactical Air Command, Langley Air Force Base (TPL-RQD-M)
2 Aeronautical Systems Division, Wright-Patterson Air Force Base
Steering Committee Member, IRIG (1)
ASAPRD-Dist (1)
1 Air Force Electronic Systems Division, Bedford, Mass.
4 Air Force Flight Test Center, Edwards Air Force Base
Steering Committee Member, IRIG (1)
Members, Optical Systems Working Group, IRIG (2)
Member, Electromagnetic Propagation Working Group, IRIG (1)
1 Air Force Missile Development Center, Holloman Air Force Base
6 Air Force Missile Test Center, Patrick Air Force Base
Steering Committee Member, IRIG (1)
Members, Electromagnetic Propagation Working Group, IRIG (2)
Members, Optical Systems Working Group, IRIG (2)
Technical Information and Intelligence Office, MTOI (1)
4 Air Proving Ground Center, Eglin Air Force Base (Members, Optical
Systems Working Group, IRIG)
5 Eglin Air Force Base
Steering Committee Member, IRIG (1)
Member, Optical Systems Working Group (2)
Member, Electromagnetic Working Group (2)
2 Holloman Air Force Base
Member, Optical Systems Working Group, IRIG (1)
Member, Electromagnetic Propagation Working Group, IRIG (1)
1 Rome Air Development Center, Griffiss Air Force Base
1 Assistant Secretary of Defense (R & E)(Member, Steering Committee, IRIG)
10 Armed Services Technical Information Agency (TIPCR)
3 National Aeronautics and Space Administration
Steering Committee Member, IRIG (1)
Member, Electromagnetic Propagation Working Group, IRIG (1)
Member, Optical Systems Working Group, IRIG (1)
2 National Bureau of Standards
Office of Basic Instrumentation (1)
Steering Committee Member, IRIG (1)
1 Applied Physics Laboratory, JHU, Silver Spring (Technical Document Center)
1 AVCO Research Laboratory, Everett, Mass. (Document Control Center)
1 California Institute of Technology, Pasadena (Library)
2 General Dynamics, Pomona, Calif. (Missile Division)
1 Harvard College Observatory, Cambridge, Mass.
1 Jet Propulsion Laboratory, CIT, Pasadena
1 Lick Observatory, Mt. Hamilton, Calif.
1 Lincoln Laboratory, MIT, Lexington
1 Lowell Observatory, Flagstaff, Ariz.
2 Massachusetts Institute of Technology, Cambridge
Research Laboratory of Electronics (1)
Servomechanisms Laboratory (1)